LA–12955-MS

LIBRARY COPY

TA-33

Landslides and Other Mass Movements Near Technical Area 33, Los Alamos National Laboratory

LANL
G / M / TR/95

4720

Los Alamos
NATIONAL LABORATORY

Los Alamos National Laboratory is operated by the University of California for the United States Department of Energy under contract W-7405-ENG-36.

Edited by Joshua Smith, Bethco Inc., for group CIC-1

Cover photo: White Rock Canyon below TA-33, looking downriver. The lower end of Chaquehui Canyon is at the bend in the Rio Grande in the distance. Cliffs in middle of photo expose Tshirege Member Bandelier Tuff overlying basaltic andesite and basalts of the Cerros del Rio volcanic field. Photo is taken from east edge of TA-33 slump blocks.

An Affirmative Action/Equal Opportunity Employer

This report was prepared as an account of work sponsored by an agency of the United States Government. Neither The Regents of the University of California, the United States Government nor any agency thereof, nor any of their employees, makes any warranty, express or implied, or assumes any legal liability or responsibility for the accuracy, completeness, or usefulness of any information, apparatus, product, or process disclosed, or represents that its use would not infringe privately owned rights. Reference herein to any specific commercial product, process, or service by trade name, trademark, manufacturer, or otherwise, does not necessarily constitute or imply its endorsement, recommendation, or favoring by The Regents of the University of California, the United States Government, or any agency thereof. The views and opinions of authors expressed herein do not necessarily state or reflect those of The Regents of the University of California, the United States Government, or any agency thereof.

LA-12955-MS

UC-903
Issued: June 1995

Landslides and Other Mass Movements Near Technical Area 33, Los Alamos National Laboratory

Steven L. Reneau
*David P. Dethier**
John S. Carney

**Department of Geology*
Williams College, 880 Main Street
Williamstown, Massachusetts, 01267-2684

Los Alamos
NATIONAL LABORATORY

Los Alamos, New Mexico 87545

Contents

Introduction 3
Setting 4
Bedrock Geology 5
- Santa Fe Group 5
- Puye Formation 5
- Pliocene Fluvial and Lacustrine Deposits 8
- Cerros del Rio Volcanic Field 8
  - Mafic Lavas 8
  - Phreatomagmatic Deposits 9
  - "Pajarito Plateau" Tholeiitic Basalt 10
- Otowi Member Bandelier Tuff 10
- Early Quaternary Alluvium 11
- Tshirege Member Bandelier Tuff 12
- Faults 13

Landslides and Other Mass Movements 14
- Introduction 14
- Causes of Landslides 18
- Slump Complexes 18
- Rock Avalanches 21
- Translational Landslides 22
- Rockfalls 22
- Gullies 23

Landslide-Dammed Lakes 23
- Oldest Lake (≥ 43 ka) 23
- Intermediate Lake (≤ 17.5 ka) 29
- Youngest Lakes (≤ 13.7 ka to ≤ 12.4 ka) 29
- Effects of Lake Drainage 33
- Causal Factors 36

Long-Term Evolution of White Rock Canyon 37
Implications for Potential Slope Instability at MDAs 42
- Influence of Rock Type on MassWWasting 42
- Local Susceptibility to Mass-Wasting 43
- Timing of Mass-Wasting 43
- Summary 44

Acknowledgments 45
References Cited 45

List of Figures

Fig. 1–Map showing geographic features along White Rock Canyon 3

Fig. 2–(A) Photograph of White Rock Canyon below TA-33 (B) Photograph of fanglomerate facies of Puye Formation 6

Fig. 3–Relationships among bedrock units exposed in the vicinity of White Rock Canyon 7

Fig. 4–Stratigraphic sections in (A) lower Ancho Canyon and (B) south of lower Chaquehui Canyon 7

Fig. 5–Geologic cross-sections through MDAs at TA-33 9

Fig. 6–Map showing approximate course of early Quaternary Rio Grande 11

Fig. 7–Plot of (A) width and (B) depth of modern White Rock Canyon and early Quaternary Rio Grande canyon 12

Fig. 8–Approximate correlation of mapping units within the Tshirege Member 13

Fig. 9–East-west transect along the rim of White Rock Canyon, showing Quaternary faults 14

Fig. 10–Photographs of slumps along western side of White Rock Canyon 15

Fig. 11–Map showing location of landslide zones and rock avalanche deposits 16

Fig. 12–Cross-sections of landslides 19

Fig. 13–Plots of distance from rim of White Rock Canyon to Holocene Rio Grande surfaces 20

Fig. 14–Plots of average slope gradient in White Rock Canyon 21

Fig. 15–Map showing location of lacustrine deposits and radiocarbon dated sites 24

Fig. 16–Diagram showing inferred water level in the Chino Mesa/Water Canyon West area 25

Fig. 17–Sketch of stratigraphic section near the mouth of Cañada Ancha 27

Fig. 18–Photographs of laminated lacustrine sediments 28

Fig. 19–Sketch map of Water Canyon West-Chino Mesa landslide dam area 30

Fig. 20–Schematic cross-section through Water Canyon West-Chino Mesa landslide dam area 30

Fig. 21–Sketch of stratigraphy showing radiocarbon sample sites below Chino Mesa 31

Fig. 22–Cross-sections of Red Dot Trail area 32

Fig. 23–Cross-sections of Blue Dot Trail area 34

Fig. 24–Measured stratigraphic sections exposed in Red Dot Trail area 35

Fig. 25–Measured stratigraphic section exposed near the Blue Dot Trail area 35

Fig. 26–Schematic long-term evolution of northern White Rock Canyon area 38

Fig. 27–Plot of canyon width vs. canyon depth 41

Fig. 28–(A) Approximate varations in stratigraphy along northwest side of White Rock Canyon. (B) Estimated time of initiation of major slump landslides (C) Rim-to-floodplain distance. (D) Estimated rim retreat rate 41

List of Tables

Table 1–$^{40}Ar/^{39}Ar$ dates from TA-33 area ____ 10

Table 2–Selected characteristics of landslide zones along northern White Rock Canyon ____ 17

Table 3–Radiocarbon dates from White Rock Canyon ____ 26

Table 4–Averaged radiocarbon dates from White Rock Canyon ____ 31

Table 5–Possible time of initiation of major slump landslides ____ 40

LANDSLIDES AND OTHER MASS MOVEMENTS NEAR TECHNICAL AREA 33, LOS ALAMOS NATIONAL LABORATORY

by

Steven L. Reneau, David P. Dethier, and John S. Carney

ABSTRACT

Massive slump complexes and at least two rock avalanches flank the eastern rim of the Pajarito Plateau along northern White Rock Canyon, north of Technical Area 33 (TA-33). The slumps failed along mechanically weak rocks in the Santa Fe Group, in the Puye Formation, or in Pliocene alluvial and lacustrine units. These rock units are not exposed beneath Material Disposal Area E (MDA-E), and therefore exposure of wastes at MDA-E due to the initiation of slumps is improbable. In contrast, rock units susceptible to slumping apparently underlie MDA-D, and the presence of relatively steep canyon walls below MDA-D suggests a relatively high susceptibility to future failure. Initiation of new slumps by the failure of the canyon rim is infrequent in White Rock Canyon, and the major slumps are mainly older than 58 ka (thousands of years ago). The toe area of at least one slump complex has been active in the late Pleistocene, damming the Rio Grande near the mouth of Water Canyon at least four times during the period from 18 to 12 ka and producing lakes that may have extended upriver to Otowi bridge. An earlier landslide-dammed lake, ≥ 43 ka in age, extended past Otowi bridge and possibly upriver to Española. The development of the youngest landslide-dammed lakes during a period of significantly wetter climate suggests that initiation of new landslides that might affect MDA-D would require a major climate change with greatly increased precipitation.

Rockfall and headward erosion of gullies do not represent significant decadal hazards on canyon rims near TA-33. In addition, gully-head migration near MDA-K is restricted to erodible soils and should not affect contaminants contained within tuff, although erosion and transport of contaminated soils is possible. A system of north-to-northeast-trending faults, some of which display Quaternary activity, bisects the TA-33 mesa. These faults are a potential source of earthquakes that could generate local ground rupture and significant seismic shaking, although shaking at TA-33 would be more likely from other seismic sources in the region.

INTRODUCTION

Massive landslides dominate the morphology of White Rock Canyon which lies along the Rio Grande on the eastern margin of the Pajarito Plateau. The developed part of Technical Area 33 (TA-33) at Los Alamos National Laboratory (LANL) borders White Rock Canyon between Ancho and Chaquehui Canyons. Two material disposal areas (MDAs), MDA-D and MDA-E, occur within 100 m of the canyon rims at TA-33 (Fig. 1, Plate 1), and an evaluation of the potential for landslides at these sites is required for long-term risk assessment decisions. MDA-E, at South Site, is the primary site requiring information on the style and frequency of landslides. This MDA, used from 1950 to 1963, contains beryllium, uranium, and various shot debris buried within

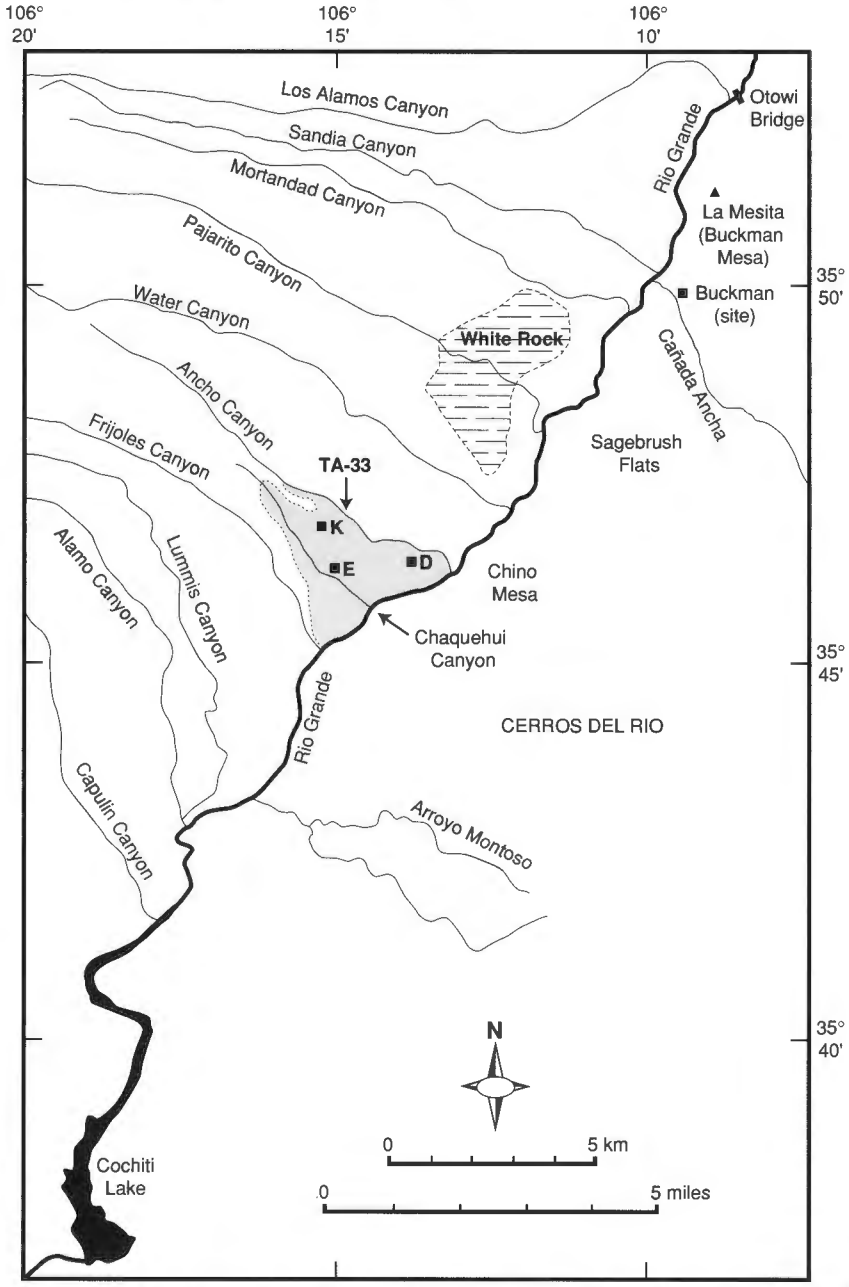

Fig. 1. Map showing geographic features along White Rock Canyon of the Rio Grande and MDAs at TA-33 (labeled D, E, and K).

pits as close as 20 m to Chaquehui Canyon cliffs (LANL, 1992). MDA-D, at East Site on the point between lower Ancho Canyon and White Rock Canyon, was active from 1948 to 1952 and includes beryllium and high explosives in underground concrete chambers that lie within 70 m of the Ancho Canyon rim and 130 m of the White Rock Canyon rim. Other potential contamination associated with firing areas active from 1955 to 1972, including uranium, ^{60}Co, tritium, lead, and cadmium, is present at East Site at similar distances from the mesa edges (LANL, 1992). A third MDA at TA-33, MDA-K, is located near the crest of the mesas west of White Rock Canyon (Fig. 1, Plate 1). MDA-K contains a septic system and leach fields for a high-pressure tritium facility, which was operational from 1955 to 1990, and contamination here includes tritium, uranium, plutonium, beryllium, mercury, and organic compounds (LANL, 1992).

This study evaluates the potential for slope instability that could affect the TA-33 MDAs and focuses on the characteristics of landslides and other mass wasting features within White Rock Canyon and the tributary canyons at TA-33. This report builds on earlier reports by Dethier (1993a, 1993b), which summarized the geology of White Rock Canyon and the initial results from the 1993 field season. The bedrock geology of White Rock Canyon is first summarized here because of the importance of lithologic variations on slope stability. The characteristics of landslides are then discussed, including spatial variations and data on the timing of failure, which provide insight into the factors influencing slope instability.

SETTING

Northern White Rock Canyon, for purposes of this report, begins at Otowi bridge and extends south along the Rio Grande to the vicinity of Chaquehui Canyon. This section of White Rock Canyon is bounded by the Pajarito Plateau to the west, the Cerros del Rio volcanic field to the east, and the broad flood plain of the Rio Grande in the Española basin to the north. Topography is steep and rugged in the canyon and along major tributaries that drain the Pajarito Plateau (Fig. 1), such as Mortandad, Water, and Ancho Canyons. Local relief ranges from 170 to more than 300 m, and cliff areas as high as 100 m are common.

Slope stability along northern White Rock Canyon is probably related to climate, particularly effective moisture, groundwater discharge, the magnitude and duration of erosive peak flows on the Rio Grande, and periods of rapid canyon cutting. The present climate in White Rock Canyon is arid to semi-arid, although it is not monitored. Immediately west of the canyon at the town of White Rock, 300 m higher in elevation, annual precipitation is about 34 cm, and mean annual temperature is about 9.5°C (Bowen, 1990); precipitation is lower and temperatures are higher within the canyon. In most years about one-half of the annual precipitation occurs during intense convective storms associated with the summer monsoon season of July and August. During the rest of the year precipitation is generally associated with the passage of frontal storms and tends to be less intense (Bowen, 1990). Peak discharge in the Rio Grande tends to occur in two periods (Nordin and Beverage, 1965; Graf, 1994). The summer storm season is characterized by peak flows of relatively short duration, whereas the snowmelt season of April to June produces sustained flows and generally higher peak discharges. Channel scour and at least local lowering of base level is thus most likely during snowmelt flows. Differences in precipitation and flood discharge that may have occurred as a result of regional climatic changes are discussed in a later section. Twenty springs that discharge from Pliocene and Miocene sedimentary rocks

have been identified along the western slopes of White Rock Canyon between Otowi bridge and Frijoles Canyon (Purtymun et al., 1980). Flow from these springs is thought to represent discharge from the main aquifer beneath the Pajarito Plateau (Purtymun et al., 1980), and presumably the discharge rate could vary with regional climatic changes, in turn affecting the stability of slopes in White Rock Canyon.

BEDROCK GEOLOGY

Cliffs and scarps of landslides along White Rock Canyon expose as much as 250 m of horizontal to slightly dipping Miocene, Pliocene, and lower Quaternary rocks (Fig. 2a). Principal units, from oldest to youngest, include sedimentary rocks of the Santa Fe Group, volcaniclastic and quartzite-rich gravels of the Puye Formation, older alluvial deposits, basaltic flows and phreatomagmatic deposits of the Cerros del Rio volcanic field, and the lower and upper Bandelier Tuff (Griggs, 1964; Dethier, 1995). Figure 3 shows the interfingered relationships among the bedrock units near the northern end of White Rock Canyon, and these units near TA-33 are mapped on Plate 1. Each of the bedrock units is incorporated, at least locally, into the massive landslides that flank the Rio Grande. Most failure surfaces are apparently within the Santa Fe Group, Pliocene alluvium and lacustrine deposits, or volcanic deposits within the Puye Formation. The stratigraphy and selected characteristics of these units are summarized below.

Santa Fe Group

The Miocene Santa Fe Group exposed in White Rock Canyon is composed primarily of pinkish-grey to buff-colored, poorly to moderately lithified silty sandstone and pebbly sand with an arkosic matrix (unit Tsfu of Plate 1) (Dethier, 1995; see also Griggs, 1964; Galusha and Blick, 1971). Thin beds of altered dacitic tephra are locally abundant. These rocks record mainly fluvial deposition on the distal margins of alluvial fans constructed when the Española basin was internally drained. The sandstone, locally cemented with sparry calcite, crops out extensively near the Buckman townsite (Fig. 1), but is poorly exposed west of the Rio Grande. The southernmost exposure in northern White Rock Canyon is within Ancho Canyon (Fig. 4a, Plate 1). These rocks are very susceptible to failure along the Rio Grande, and landslides obscure the Miocene rocks along most of White Rock Canyon. However, probable Santa Fe Group sediments are exposed within landslides in Ancho Canyon, north of Pajarito Canyon, and elsewhere, indicating that they are widely distributed.

Puye Formation

The Puye Formation is principally a Pliocene volcanogenic alluvial fan sequence derived from the Jemez Mountains (Waresback and Turbeville, 1990), but it includes ancestral Rio Grande gravels and lacustrine deposits, particularly along and west of White Rock Canyon (Fig. 3). Following Dethier (1995), the Puye Formation is informally divided here into a fanglomerate facies (Tpf of Plate 1; Fanglomerate Member of Griggs, 1964) and an axial Rio Grande facies (Tpt of Plate 1; Totavi Lentil of Griggs, 1964; and Totavi Formation of Waresback and Turbeville, 1990). Along White Rock Canyon and tributary canyons south of Otowi bridge, these facies are interfingered laterally and in vertical sequences, although Griggs (1964) reported the Totavi Lentil only at the base of the Puye Formation. The fanglomerate facies is mainly pinkish-grey to grey, locally cemented, weakly lithified pebble-to-boulder size gravel, boulder-rich debris flows, and sand. Highly weathered dacitic pumice-rich layers also occur, and these in part

A

B

Fig. 2. (A) Photograph of White Rock Canyon below TA-33, looking downriver. The lower end of Chaquehui Canyon is at the bend in the Rio Grande in the distance. Cliffs in middle of photo expose Tshirege Member Bandelier Tuff overlying basaltic andesite and basalts of the Cerros del Rio volcanic field. Photo is taken from east edge of TA-33 slump blocks. (B) Photograph of fanglomerate facies of Puye Formation exposed in lower Water Canyon, along Water Canyon East slump complex. White layer is pumice that has weathered to clay and is deformed along landslide failure plane.

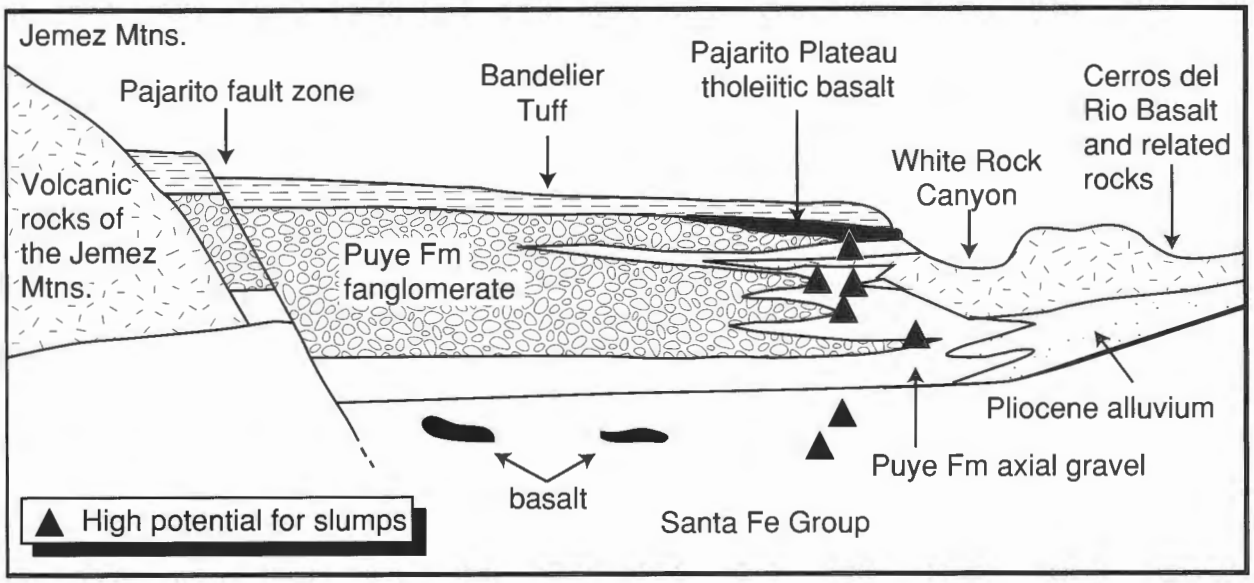

Fig. 3. Relationships among bedrock units exposed in the vicinity of White Rock Canyon (modified from Waresback and Turbeville, 1990).

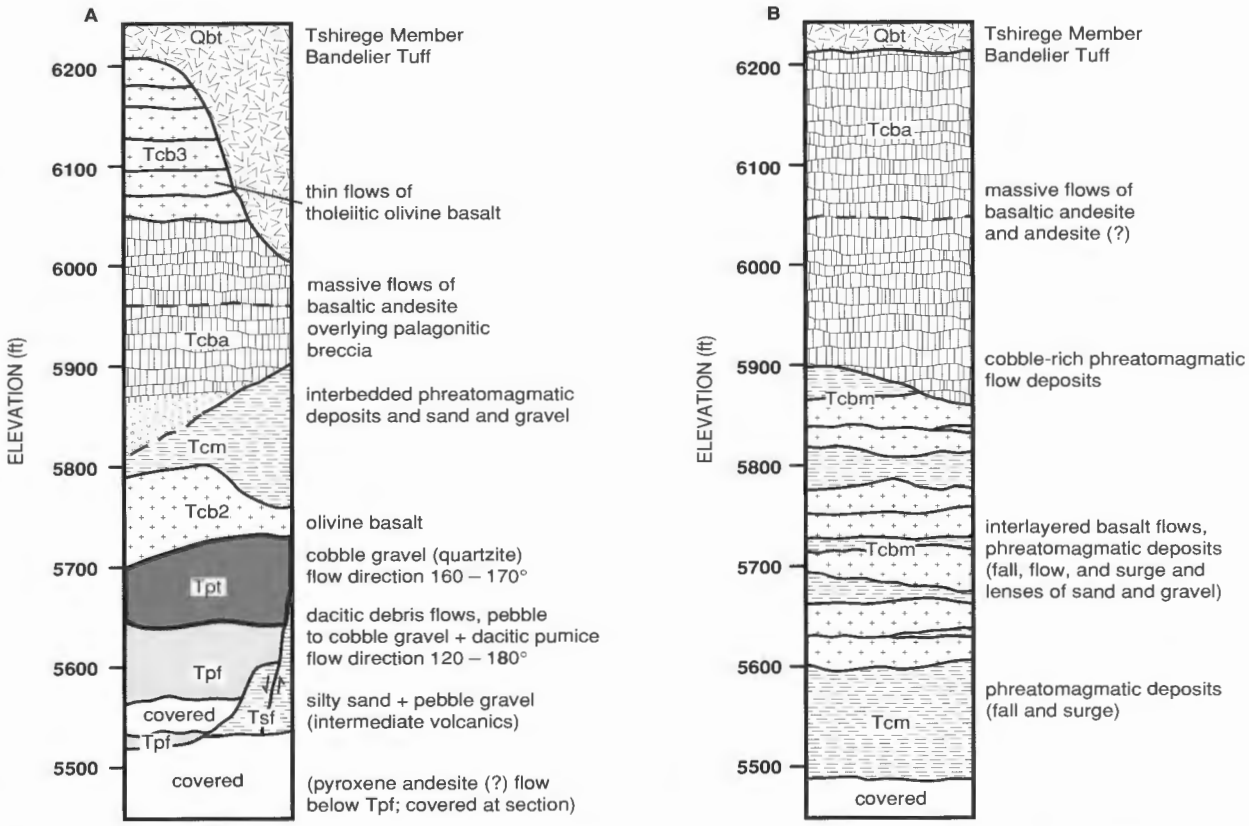

Fig. 4. Stratigraphic sections in (A) lower Ancho Canyon and (B) south of lower Chaquehui Canyon. Tcb3, Tcba, Tcm, Tcbm, and Tcb2 are lavas and related deposits of the Cerros del Rio volcanic field. Tpt and Tpf are the axial Rio Grande facies and the fanglomerate facies of the Puye Formation, respectively. Tsf is Santa Fe Group (faulted in Ancho Canyon). Modified from Dethier (1995).

serve as landslide failure planes along the north side of lower Water Canyon (Fig. 2b). These pumice layers have weathered to clay, causing a major decrease in strength, although the type of clay has not been determined. The ancestral Rio Grande facies is mainly grey, poorly to moderately lithified, locally cemented quartzite-rich pebble-to-cobble gravel, but it includes beds of silt and silty sand. In Ancho Canyon, below MDA-D, the Puye Formation is at least 60 m thick, including 25 m of Rio Grande gravels underlain by at least 35 m of fanglomerate (Fig. 4a).

Pliocene Fluvial and Lacustrine Deposits

Unlithified and generally uncemented Pliocene sedimentary deposits that are interlayered with basalt flows and phreatomagmatic deposits are exposed within a few kilometers of the Rio Grande. These rocks include buff to brownish-yellow sand and pebbly sand, silt, silty sand, and beds of cinders and debris flows. They are the temporal equivalent, in part, of the ancestral Rio Grande facies of the Puye Formation, but the presence of granitic clasts indicates that they were derived from the southern Sangre de Cristo Range (Dethier, 1994). They correlate with the older alluvium of Griggs (1964) and, in part, with the Ancha Formation of Spiegel and Baldwin (1963). Fine-grained units are locally rich in swelling clays that were probably produced from the alteration of basaltic glass derived from Cerros del Rio volcanism. Lacustrine deposits record a Rio Grande dammed south of Water Canyon contemporaneous with eruptions from maars and emplacement of basaltic flows. Subhorizontal failure planes associated with clay-rich lacustrine sediments have produced many of the complex landslides near the mouth of Mortandad Canyon and northwest and southwest of Otowi bridge, the latter involves overlying Bandelier Tuff.

Cerros del Rio Volcanic Field

Mafic Lavas. Lava flows of basalt, hawaiite, basaltic andesite, andesite, and related intrusive rocks of the Pliocene Cerros del Rio volcanic field form surface exposures along White Rock Canyon and east of the Rio Grande from Otowi bridge to Cochiti Dam. These rocks are included within units Tcc, Tcba, Tcbm, Tcb2, Tcb1, and Tcbu on Plate 1 and in Fig. 4. Volcanic landforms include maars, shields, fissure vents, cinder cones near the Rio Grande, and a cinder cone near MDA-K at TA-33 (Fig. 5a). Near Otowi bridge, mesa-capping flows are about 40 m thick, whereas south of Water Canyon the flow sequence is greater than 80 m thick and near Chaquehui Canyon massive flows are greater than 120 m thick (Fig. 4b). East of the Rio Grande, the sequence of basaltic flows also thickens to the south. The thickest flows appear to fill paleovalleys or craters greater than 60 m deep, whereas some of the thinner flows apparently spread out over surfaces of little relief. Flow bases are smooth to rubble-rich; locally a few tens of centimeters to a few meters of alluvium separates flows.

Ages of 2.3 to 2.7 Ma (millions of years ago) have been obtained from rocks of the Cerros del Rio volcanic field near northern White Rock Canyon, including $^{40}Ar/^{39}Ar$ ages of 2.4 to 2.6 Ma from basalt flows and dikes at the TA-33 cinder cone (Table 1; Fig. 5a) (Laughlin et al., 1993; Dethier, 1995). Interestingly, a topographically low flow in lower Water Canyon yielded a similar age of about 2.47 Ma (Table 1), suggesting that there was a relatively short period of intense volcanism and over 200 m of local aggradation at about 2.4 to 2.5 Ma. Basaltic lava flows are involved in most of the massive slumps that dominate the morphology of White Rock Canyon. The flow sequences often remained coherent as they were back-tilted along steep failure planes, and flow areas as extensive as hundreds of square meters held together during the >250 m of

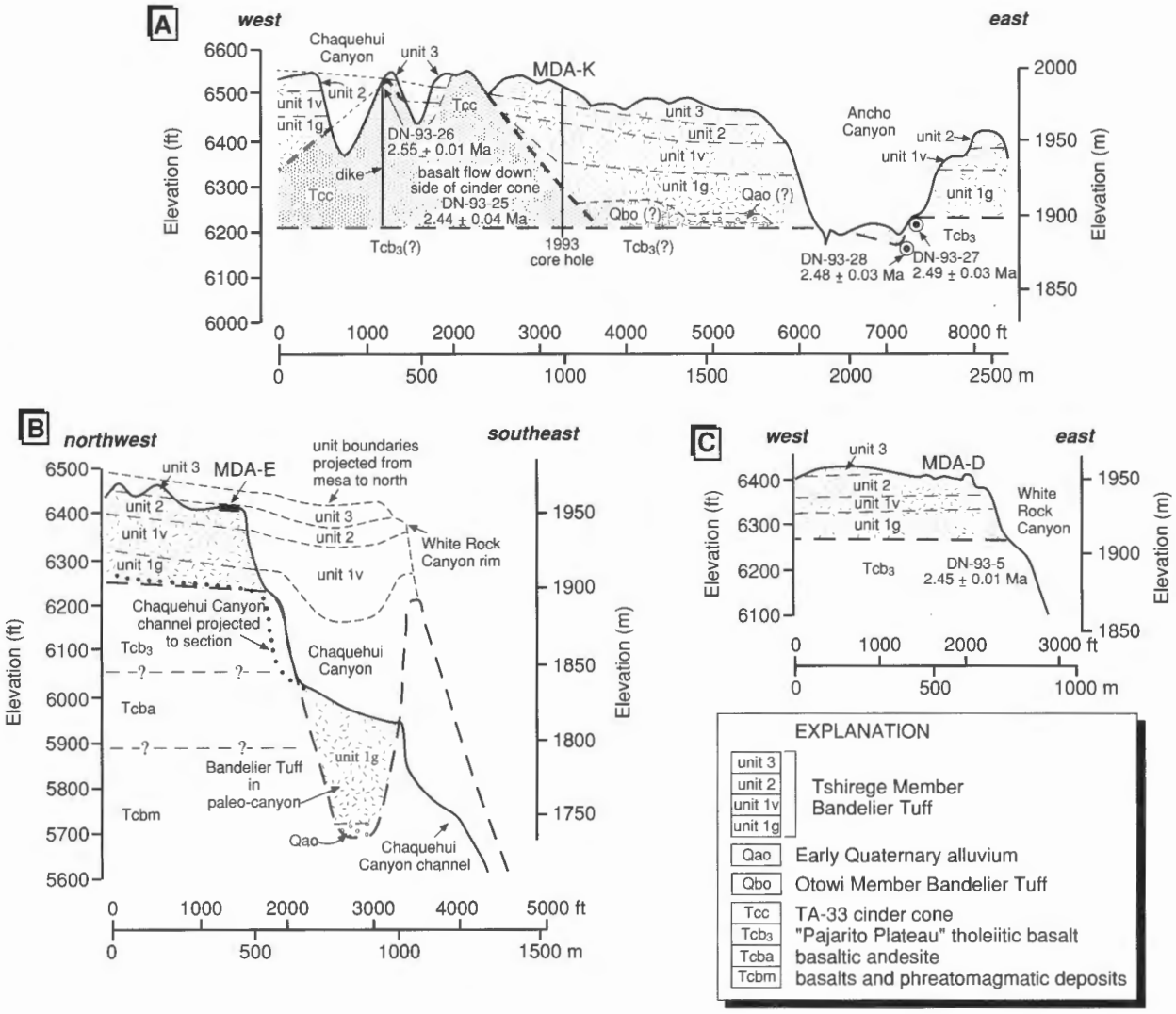

Fig. 5. Geologic cross-sections through MDAs at TA-33, showing 5x vertical exaggeration. (A) MDA-K; N81W-S81E orientation. Contacts between units 2 and 1v, 1v and 1g, 1g and Tcc, and Tcc and Tcb3 in 1993 core holes provided by A. W. Laughlin. Contact between units 3 and 2 in core holes inferred from geologic mapping. Sample numbers and dates are $^{40}Ar/^{39}Ar$ analyses from Laughlin et al. (1993). (B) MDA-E; N40W-S40E orientation. Approximate boundaries between Pliocene volcanic units from Dethier (1995). (C) MDA-D; N85W-S85E orientation.

vertical movement from the canyon rim to the edge of the Rio Grande. In other areas, where jointing is more extensive, or perhaps where failures occurred more rapidly, only basaltic rubble remains.

Phreatomagmatic Deposits. Thin-bedded to massive matrix-supported flow and fall deposits crop out at La Mesita, along Chino Mesa, between Chaquehui Canyon and Water Canyon, and in several other zones south to Cochiti Dam, mainly along the Rio Grande (units Tcm and Tcbm of Plate 1 and Fig. 4). These deposits were produced at maar volcanoes that formed when rising magmas reacted with groundwater along the Pliocene course of the Rio Grande (Aubele, 1978; Dethier, 1995; Heiken et al., 1995). At several of these volcanic centers, lava flows are interlayered with the upper

TABLE 1
$^{40}AR/^{39}AR$ AGES FROM TA-33 AREA *

Sample Number	Bedrock Unit	Isochron Age (Ma)	Location
DN-93-5	Tcb3	2.45 ± 0.01	TA-33, White Rock Canyon Rim, SW of MDA-D
DN-93-8	Tcba	2.33 ± 0.27	TA-70, White Rock Canyon Rim, at powerlines
DN-93-14	Tcb1	2.47 ± 0.03	TA-70, lower Water Canyon, near Rio Grande
DN-93-25	Tcc	2.44 ± 0.04	TA-33, basalt flow on S. side of cinder cone
DN-93-26	Tcc	2.55 ± 0.01	TA-33, dike on W. side of cinder cone
DN-93-27	Tcb3	2.49 ± 0.03	TA-70, Ancho Canyon, basalt above step
DN-93-28	Tcb3	2.48 ± 0.06	TA-70, Ancho Canyon, basalt below step

Notes:
* Samples collected as part of this study. Ages and chemical data for samples presented in Laughlin et al. (1993). $^{40}Ar/^{39}Ar$ analyses performed at New Mexico Geochronology Research Laboratory in Socorro. Uncertainty is 1 standard deviation.

portions of the phreatomagmatic sequences and some maars probably were the source of thick flows of basaltic andesite (Dethier, 1995). For instance, 30 m of phreatomagmatic deposits along the southwest side of Chaquehui Canyon near the Rio Grande are overlain by a 60-m-thick volcanic section that includes seven flows and interlayered phreatomagmatic deposits; these rocks are in turn capped by a package of flows 120 m thick that may reflect a single cooling unit (Fig. 4b). Where phreatomagmatic sequences lie above Santa Fe Group deposits or Pliocene alluvium, they are involved in massive landslides such as those exposed on the northwest flank of La Mesita. Phreatomagmatic deposits appear relatively stable where they are exposed along White Rock Canyon to the south and west of Chino Mesa, where the Santa Fe Group and Pliocene alluvium are not exposed, although phreatomagmatic deposits may in part comprise failure planes for slumps along the eastern side of TA-33 near MDA-D.

"Pajarito Plateau" Tholeiitic Basalt. Thin flows of tholeiitic basalt typically form the western rim of White Rock Canyon in the TA-33 area, extending north to Los Alamos Canyon (Dethier, 1994; unit Tcb3 of Plate 1 and Figs. 4 and 5). The flows were derived from vents to the west and northwest of White Rock, and one of these vents is exposed south of Pajarito Canyon, southwest of the intersection of Pajarito Road and State Route 4. In late Pliocene time, the basalts entered a lake dammed in White Rock Canyon at an elevation of about 6200 ft. Deltas of pillow basalt and palagonitic breccia formed at the edge of the paleolake and are best exposed in Los Alamos and Mortandad Canyons. Available data indicate that these tholeiitic flows can be distinguished from other Cerros del Rio lavas by their chemistry (Laughlin et al., 1993; Dethier, 1995) in addition to their higher stratigraphic position and flow direction. Ages of 1.8 to 2.5 Ma have been obtained from these basalts (Luedke and Smith, 1978; Laughlin et al., 1993; Dethier, 1995), including $^{40}Ar/^{39}Ar$ ages of 2.45 to 2.49 Ma near TA-33 (Table 1; Fig. 5a).

Otowi Member Bandelier Tuff

The Otowi Member of the Bandelier Tuff consists of light-grey, nonwelded pyroclastic flows of pumiceous rhyolite and a basal pumiceous fall unit, the Guaje Pumice Bed (Bailey et al., 1969). The Otowi Member was erupted from the Jemez Mountains about 1.6 Ma (Izett and Obradovich, 1994). Only the Guaje Pumice Bed is widely preserved

near White Rock Canyon, where it lies unconformably on surfaces cut into Pliocene basalt of the Cerros del Rio or on Pliocene alluvium. Near TA-33, small exposures of the Otowi Member are present in Ancho Canyon near State Route 4, and the Otowi Member is also exposed further down Ancho Canyon within a pre-Bandelier Tuff paleocanyon (Plate 1), possibly in an ancient cut-off meander bend.

Early Quaternary Alluvium

Early Quaternary alluvium is locally exposed near TA-33 below the Tshirege Member of the Bandelier Tuff. Volcanic fall-out units of the Cerro Toledo Rhyolite, which fill this stratigraphic interval to the northwest (Heiken et al., 1986), are apparently sparse in the vicinity of White Rock Canyon. In Ancho Canyon near State Route 4 (Plate 1), about 6 m of dacite-rich bouldery stream gravels derived from a stream draining the Sierra de los Valles occur between the Otowi and Tshirege Members. In lower Water Canyon and a northeastern tributary to lower Ancho Canyon, alluvial deposits composed largely of quartzite-rich gravels and river-polished basalt boulders occur beneath the Tshirege Member and indicate that the early Quaternary position of the Rio Grande was at an elevation of about 5700 to 5800 ft (Fig. 6). The early Quaternary paleocanyon of the Rio Grande was much shallower and narrower than the modern canyon (Fig. 7), was incised largely into basalts, and was apparently unmodified by extensive slump landslides such as those occurring along the modern canyon. Between Water Canyon and Lummis Canyon, the paleochannel had an apparent gradient of about 0.0031 to 0.0036, significantly steeper than the modern Rio Grande gradient of about 0.002, assuming that the

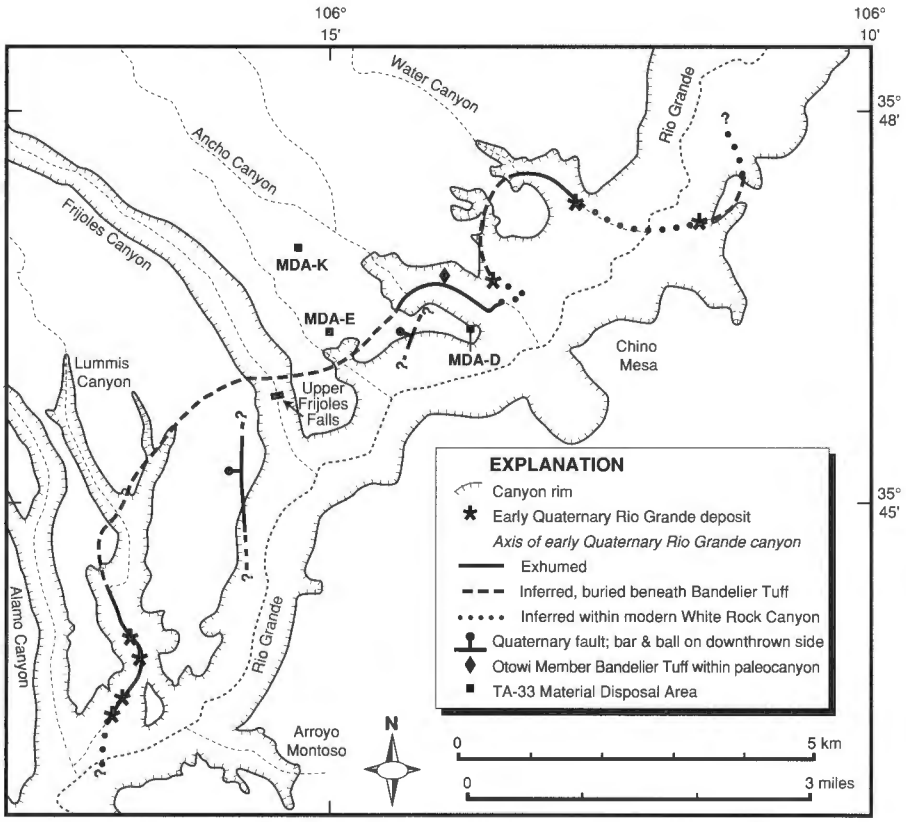

Fig. 6. Map showing approximate course of early Quaternary Rio Grande (prior to eruption of Tshirege Member Bandelier Tuff) and faults with Quaternary offset.

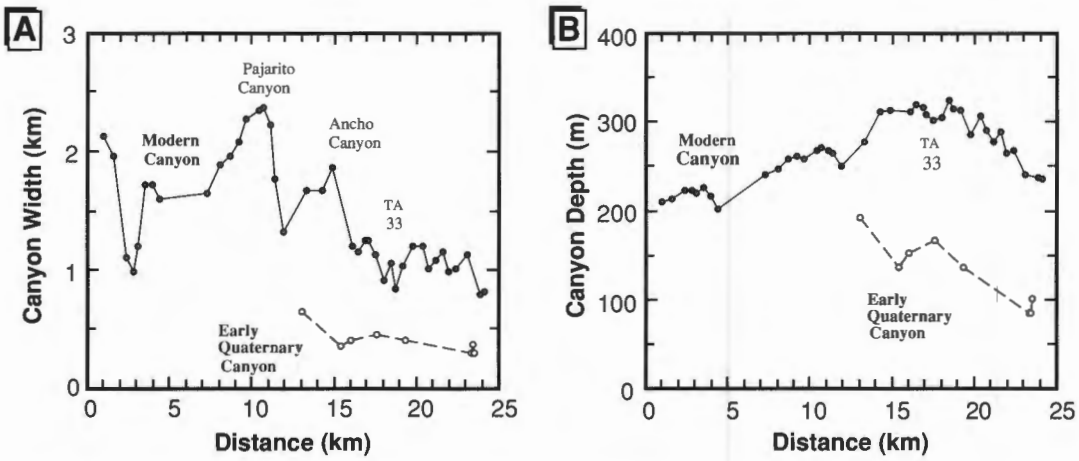

Fig. 7. Plot of (A) width and (B) depth of modern White Rock Canyon and early Quaternary Rio Grande canyon vs. distance downstream from Otowi bridge. Measurements made from canyon rims along transects perpendicular to center-line of canyon. Massive landslides dominate the wider parts of the canyon, and canyon width decreases significantly at TA-33 associated with less extensive landsliding. Canyon width and canyon depth are not correlated, except for downriver areas in basalt and for early Quaternary canyon.

paleocanyon had the sinuosity shown in Fig. 6. If the canyon was significantly more sinuous, however, then the gradients could be similar.

Tshirege Member Bandelier Tuff

The Tshirege Member of the Bandelier Tuff at TA-33 consists of light-grey nonwelded to slightly welded pumiceous pyroclastic flows and a thin basal pumiceous fall unit, the Tsankawi Pumice Bed (Bailey et al., 1969). These rocks were erupted from the Jemez Mountains about 1.22 Ma (Izett and Obradovich, 1994). The Tshirege Member is the uppermost rock unit at TA-33 and underlies the MDAs (Fig. 5). It is typically about 60 to 75 m (200 to 250 ft) thick at TA-33, but pinches out over paleotopographic highs, such as the TA-33 cinder cone, and reaches a thickness of about 230 m (750 ft) where it fills the early Quaternary paleocanyon (Fig. 5b).

The Tshirege Member can be divided into mapping units that reflect distinct flow units or cooling units and variations in alteration. Four mapping units modified from the units of Baltz et al. (1963) and Vaniman and Wohletz (1990) in other parts of the Pajarito Plateau are used in this study. These units also generally correspond with units A through D of M. A. Rogers (unpublished maps*). Approximate correlations between units are shown on Fig. 8.

The lowest unit, unit 1g, consists of nonwelded ignimbrite with glassy pumice, following Vaniman and Wohletz (1990). The second lowest unit, unit 1v, consists of nonwelded vapor-phase altered ignimbrite, also following Vaniman and Wohletz (1990). Unit 2 is the primary cliff-former at TA-33, consisting of slightly welded ignimbrite with discontinuous surge beds at the base. The contact of unit 2 with the overlying nonwelded to slightly welded ignimbrites of unit 3 is poorly defined and is here considered to be the approximate break in slope at the base of the upper, relatively steep tuff step.

The mapping boundaries used in this report are believed to be most similar to those of Baltz et al. (1963) and Rogers (unpublished) who also mapped parts of the eastern Pajarito Plateau. Some of the unit boundaries of Vaniman and Wohletz (1990) may be

*Geologic maps of Los Alamos National Laboratory by M.A. Rogers are planned for reproduction and distribution in 1995 by the New Mexico Environment Department.

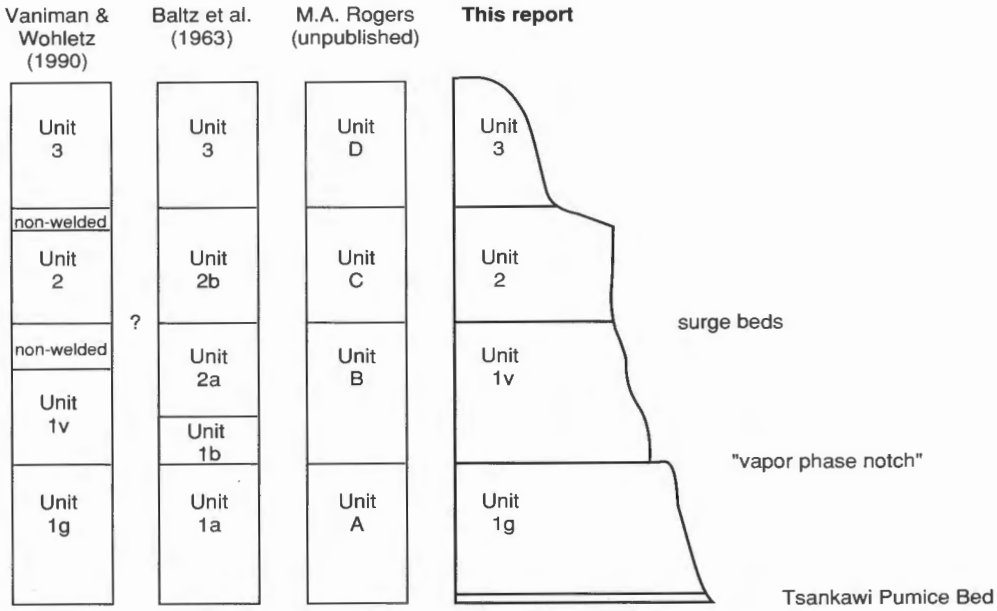

Fig. 8. Approximate correlation of mapping units within the Tshirege Member of the Bandelier Tuff used in this report with units used in other studies.

placed at different stratigraphic positions, reflecting east-to-west variations in the Tshirege Member. For example, the surge beds that mark the base of Unit 2 on the eastern plateau are not present to the west, and the base of the Vaniman and Wohletz (1990) Unit 2 may be stratigraphically lower.

Faults

Several previously unrecognized faults were found at TA-33 during this study, including a fault zone with Quaternary offset along the rim of White Rock Canyon 0.5 to 0.65 km west of MDA-D and 1.1 to 1.25 km east of MDA-E (Fig. 6; Plate 1). Two near-vertical northeast-trending faults offset surge beds at the base of Tshirege Member unit 2 by about 2.4 and 3.2 m down-to-the-northwest, and vertical striae along one of these faults indicates pure-dip slip offset (Fig. 9). An additional northwest-trending fault with about 1.8 m of down-to-the-southeast offset occurs between the northeast-trending faults, and striae again indicate dip-slip offset (Fig. 9). Cumulative down-to-the-northwest offset is about 3.8 m across this fault zone. Offset has not been recognized in Ancho Canyon along the inferred trend of the fault zone, and the northern continuation of these faults is uncertain.

At least two additional north-striking, down-to-the-west faults cut the uppermost basalts farther west along the northwestern rim of White Rock Canyon at TA-33 (Plate 1). At one of these sites, with an estimated 11 to 12 m of offset, a $^{40}Ar/^{39}Ar$ age of 2.45 Ma was obtained on the faulted basalt (sample DN-93-5, Table 1), constraining the age of the faulting. These faults may also have had Quaternary activity, but reconnaissance mapping did not indicate offset of the overlying Bandelier Tuff. An additional fault with down-to-the-west offset of the Pliocene basalt may occur in Ancho Canyon (Fig. 5a), but the potential fault surface is buried beneath colluvium and an erosional step is also possible.

An additional, previously unmapped Quaternary fault was recognized during reconnaissance mapping of White Rock Canyon southwest of TA-33. This fault, which is exposed along the canyon rim 1.1

km southwest of the mouth of Frijoles Canyon (Fig. 6), trends roughly north-south with about 20 to 25 m of apparent down-to-the-west offset of the basal contact of unit 2 of the Tshirege Member. Evidence for offset of the Bandelier Tuff along this trend has not been seen in Frijoles Canyon, and it is inferred that the offset dies out 1 to 2 km north of White Rock Canyon.

Quaternary faulting on the eastern Pajarito Plateau is significant because it demonstrates the possibility of surface rupture hazards within the eastern part of LANL, including TA-33. The predominant down-to-the-west or northwest sense of movement is consistent with faults inferred in the subsurface beneath LANL by Dransfield and Gardner (1985). The relative offsets of ~2.45-Ma basalt and 1.22-Ma Tshirege Member Bandelier Tuff suggest that faults in this area may have been significantly more active in the Pliocene than the Quaternary, perhaps associated with Pliocene Cerros del Rio volcanism. However, a thorough investigation of these faults has not been completed, and an evaluation of the potential hazard from these faults will require more detailed paleoseismic data.

LANDSLIDES AND OTHER MASS MOVEMENTS

Introduction

Pervasive landslides are among the most striking geologic features of White Rock Canyon between TA-33 and Otowi bridge. Most of these landslides initiated as slumps (Fig. 10) in which relatively intact masses of bedrock were transported along curved failure surfaces (e.g., Varnes, 1978), although the lower parts of some of these landslides may grade into earthflows or debris flows. Other significant mass-movement features include rock avalanches—in which large masses of bedrock completely disaggregated during rapid downslope movement—and translational landslides, in which movement occurred along steep, mainly planar surfaces. Small-scale rockfalls are also common in White Rock Canyon but were only examined in detail at TA-33.

Between TA-33 and Otowi bridge, a distance of about 16 km, landslides cover some 20 km^2, and the average distance between canyon rims is about 1.8 km (Fig. 7a). Landslides thus occupy roughly 70% of the area within northern White Rock Canyon. In the 20 km south of Chaquehui Canyon,

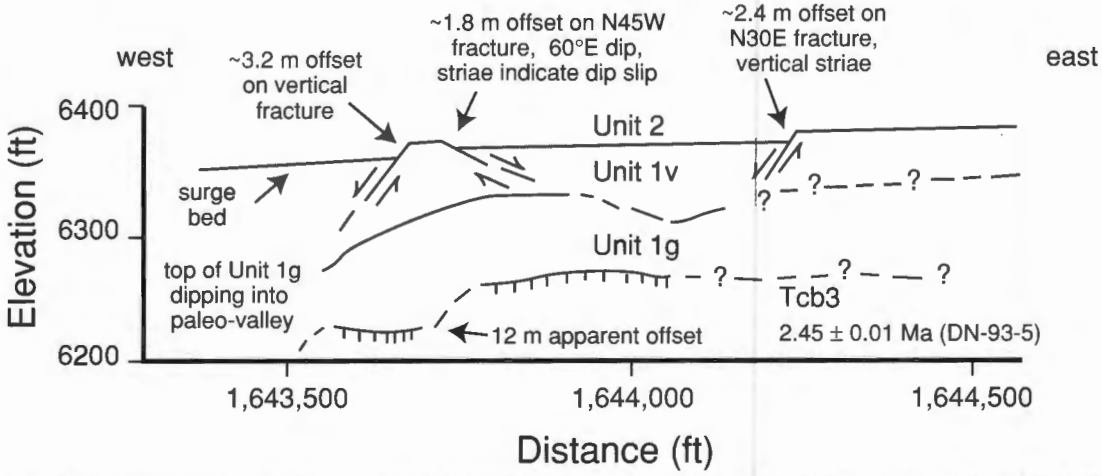

Fig. 9. Bedrock stratigraphy on an east-west transect along rim of White Rock Canyon west of MDA-D showing fault offsets of the Bandelier Tuff and Pliocene basalt. Stratigraphic markers surveyed with total station. Horizontal scale uses New Mexico State Plane coordinates (NAD 83 datum). Faults are steeply dipping, with the apparent low fault dips an artifact of the orientation of the exposure.

A

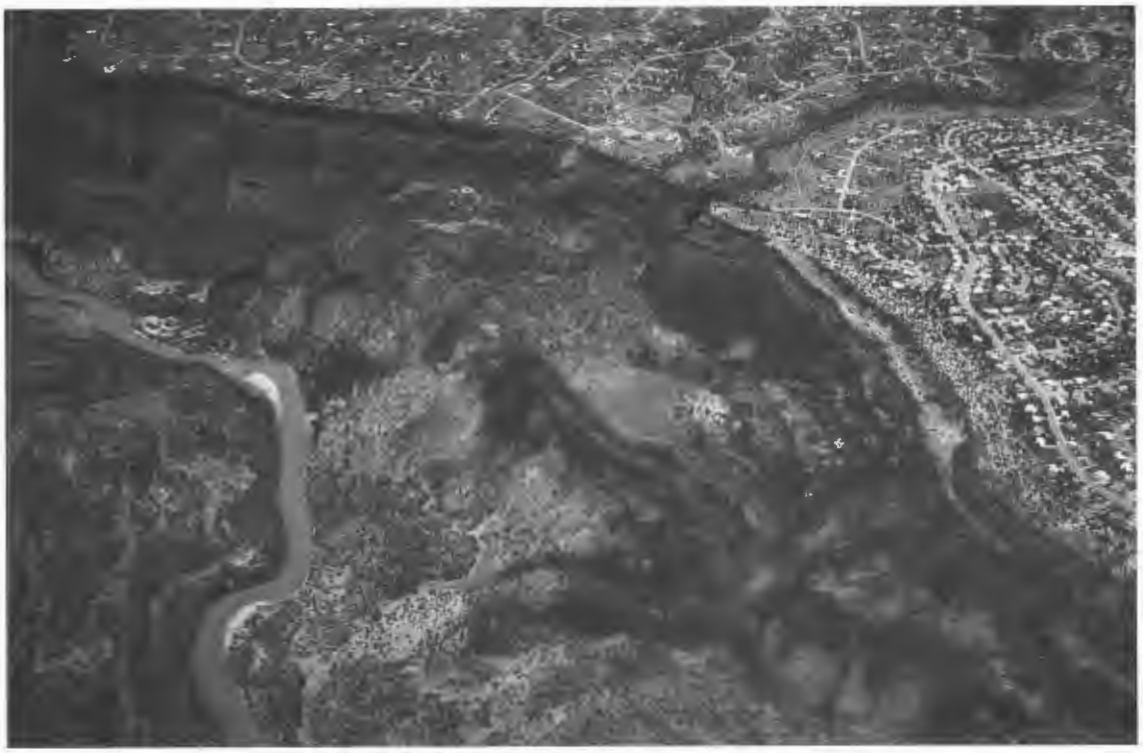

B

Fig. 10. Photographs of slumps along western side of White Rock Canyon. (A) Oblique aerial photo of Pajarito Canyon slump complex below White Rock. (B) Water Canyon West slump complex. Light colored rocks on block to left are Tshirege Member Bandelier Tuff, dipping 50° to west (right). East Site at TA-33 on right skyline.

the distance between rims averages less than 1 km and landslides cover less than 20% of this area (D.P. Dethier, unpublished mapping, 1985-86). Landslide zones between Chaquehui Canyon and Otowi bridge have been examined in reconnaissance west of the Rio Grande and can be divided into 11 general groups (Fig. 11; Table 2). Average landslide width, defined as landslide area divided by rim length, ranges from about 50 m near Chaquehui Canyon to more than 1.5 km between Ancho Canyon and Water Canyon. Landslides and other deposits in the vicinity of TA-33 and TA-70 are shown on Plate 1.

The age of individual landslides, obtained by several methods, is useful for evaluating the timing and frequency of landslide movement in White Rock Canyon. The El Cajete pumice, produced by the most recent volcanic eruptions from the Jemez Mountains, constitutes an important stratigraphic marker in the White Rock Canyon area.

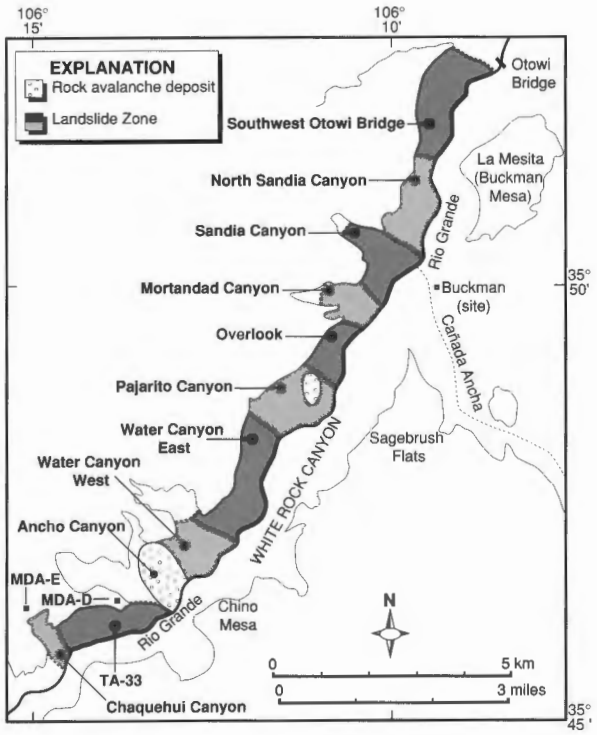

Fig. 11. Map showing location of landslide zones and rock avalanche deposits west of the Rio Grande in northern White Rock Canyon.

Conflicting ages have been obtained for the pumice and related units. Fission-track and $^{40}Ar/^{39}Ar$ analyses have indicated ages of 130 to 180 ka (thousands of years ago) and >200 ka, respectively (Self et al., 1988, 1991). Recent electron spin resonance (ESR) analyses suggest significantly younger ages of 45 to 73 ka (Toyoda et al., 1995). The ESR estimates are generally consistent with a thermoluminescence (TL) estimate of 51 ± 4 ka for the A horizon of a soil buried beneath the pumice on the Pajarito Plateau (sample OTL464, S. L. Forman, written communication, 1994)*, and radiocarbon age estimates of >58 ka from charcoal entrained within the pumice beds in the Jemez Mountains (S. L. Reneau and J. N. Gardner, unpublished data). For the purposes of this report, we will consider the age of the El Cajete pumice to be >58 ka.

Other age control used in White Rock Canyon includes radiocarbon analyses of charcoal associated with landslide-dammed lakes, soil development, and rock varnish. Radiocarbon analyses discussed in the text (obtained in this study and from other studies) are expressed in "radiocarbon years before present" (BP), which differ from calendar years as a result of temporal fluctuations in the atmospheric $^{14}C/^{12}C$ ratio. Corrections to calendar years (cal BP) can be made using computer software, such as that of Stuiver and Reimer (1993). Constraints on landslide age using soils in part relies on progressive variations in carbonate morphology with time (e.g., Birkeland, 1984; Machette, 1985). Rock varnish age estimates in White Rock Canyon (Dethier et al., 1988) rely on the cation ratio technique, although there are significant uncertainties concerning the cation ratio dating method, and potential sources of error are poorly understood (e.g., Reneau and Raymond, 1991; Watchman, 1992, 1994; Bierman and Gillespie, 1994).

*S.L. Forman, written communication. Byrd Polar Research Center, The Ohio State University, Columbus, Ohio, 43210-1002

TABLE 2
SELECTED CHARACTERISTICS OF LANDSLIDE ZONES ALONG NORTHERN WHITE ROCK CANYON

Landslide Zone	Landslide Type	Landslide Width (km) *	Dip of slump blocks	Failure Surface	Notes
Chaquehui Canyon	Rock slides (3); small slumps	0.05	--	Bandelier Tuff	Small failures, probably late Pleistocene
TA-33	Slump complex	0.51	30°-50°	Phreatomagmatic deposits (?) or Puye Fm	Slumps >300 m from rim
Ancho Canyon	Rock avalanche	1.69	--	Santa Fe Group (?)	Volume> 18 x 10^6 m^3
Water Canyon West	Slump complex	1.87	~50°	Puye Fm or Santa Fe Group	Blocks > 300 m wide. SE slump blocks active in late Pleistocene. Dam and spillway area for late Pleistocene lakes
Water Canyon East	Slump complex	0.57	30°-70°	Puye Fm. or Santa Fe Group	Slump blocks along Rio Grande may have been active in late Pleistocene
Pajarito Canyon	Slump complex; small rock avalanche	0.87	30°-70°	Puye Fm. or Santa Fe Group	Largest slump block >300 x 500 m
Overlook	Slump complex	0.61	10° (near rim) to 70° near river	Puye Fm or Pliocene alluvium	Slump blocks <150 m wide; locally 50 m
Mortandad Canyon	Slump complex	0.22	10°-30°	Pliocene alluvium	Failure planes subhorizontal
Sandia Canyon	Slump complex	0.51	30°-50°	Pliocene alluvium and Santa Fe Group	
N. Sandia Canyon	Slump complex	0.45	30°-70°	Pliocene alluvium and Santa Fe Group	3 or 4 tiers of coherent slumps
SW Otowi Bridge	Slump complex	0.53	30°-70°	Pliocene alluvium and Santa Fe Group	3 or 4 tiers of coherent slumps locally

Notes:

*Landslide width defined as landslide area divided by rim length, and represents average width of landslide zone measured perpendicular to the canyon rim.

Causes of Landslides

Landslides are triggered when the shear stress (driving force) in slope-forming materials exceeds their shear strength (resisting force) (e.g., Varnes, 1978; Selby, 1982). Important variables that influence shear stress and shear strength in a slope include slope gradient, soil or rock strength properties (angle of internal friction and cohesion), and water pressures related to water table height and groundwater flow. Decreases in slope stability leading to failure can be caused by either gradual or rapid changes in these variables.

Variations in the shear strength of rock have a major influence on the location of slope instability, and mechanically weak rocks in White Rock Canyon such as the Pliocene lacustrine sediments and layers of clay-rich altered volcanic rock may be particularly susceptible to failure. Progressive exposure of these sedimentary rocks over time, caused by the long-term incision of the Rio Grande, has resulted in gradual decreases in the stability of the canyon walls and has been a main contributing factor in the generation of landslides in White Rock Canyon. On shorter time scales, an important triggering mechanism has probably been the removal of lateral support at the base of slopes, such as by stream erosion or landslides. Shear stresses in a slope can also be increased by increasing seepage pressures, such as by increasing groundwater discharge rates. Climate changes that have affected groundwater flow may thus have contributed to landslides near TA-33. In addition, rises in regional and perched water tables act to reduce shear strength in slope forming materials, further contributing to instability. Sudden, transitory increases in shear stress also accompany earthquakes, and the triggering of landslides by earthquakes is well documented in many areas (e.g., Keefer, 1984; Keefer and Wilson, 1989; Jibson and Keefer, 1993); late Quaternary earthquakes along the Pajarito fault system (e.g., Gardner and House, 1987; Gardner et al., 1990; Wong et al., 1993) or on other faults in the region may have been responsible for some of the failures observed within White Rock Canyon. Finally, formation and sudden draining of lakes may also have acted as short-term triggers for some landslide activity in White Rock Canyon, as discussed in a later section.

Slump Complexes

Most landslides along northern White Rock Canyon are part of extensive slump complexes that are covered with basaltic boulders and flanked by colluvium and talus. These landslides are best exposed between Ancho and Pajarito Canyons and typically consist of large slump blocks with coherent internal stratigraphy near canyon rims and progressively more deformed slumps that grade into debris flows closer to the Rio Grande (Figs. 12a and 12c; Table 2). Slump complexes become smaller south of Ancho Canyo and are limited features of the landscape south of Chaquehui Canyon. Dips in slump blocks range from 8 to 70°. Many of the slump complexes consist of individual blocks separated by scarps that may have formed at different times, recording successive failures of the landslides. The eastern edge of the Water Canyon West slump complex (Figs. 11 and 12c; Plate 1), for instance, includes several individual slumps that were active in late Pleistocene time (<20 ka), as discussed in a later section, whereas the larger slumps immediately west were emplaced before deposition of the El Cajete pumice (>58 ka). Closed depressions and back-tilted surfaces of slump blocks in many slide complexes are sites of fluvial, colluvial, and eolian deposition and are separately mapped by Dethier (1995) and on Plate 1.

The largest slump complexes on the northwest side of White Rock Canyon, corresponding to areas with the largest distances from the canyon rim to the Rio Grande

floodplain on Fig. 13a, are the Pajarito Canyon, Water Canyon West, Sandia Canyon North, and Southwest Otowi Bridge areas (Fig. 11). The largest slump complexes on the southeast side of the canyon are below Sagebrush Flats and south of Otowi bridge (Fig. 13b). In these areas, retreat of the canyon rims associated with landsliding has reduced the average canyon slope gradient to about 0.2 to 0.3, contrasting with intervening areas with gradients of as much as 0.5 to 0.6 (Fig. 14). Such reductions in slope gradient, by reducing the local shear stress, should tend to reduce the potential for additional massive slumping of the canyon rim. In addition, displaced slump masses tend to buttress lower slopes, further increasing stability until the landslide

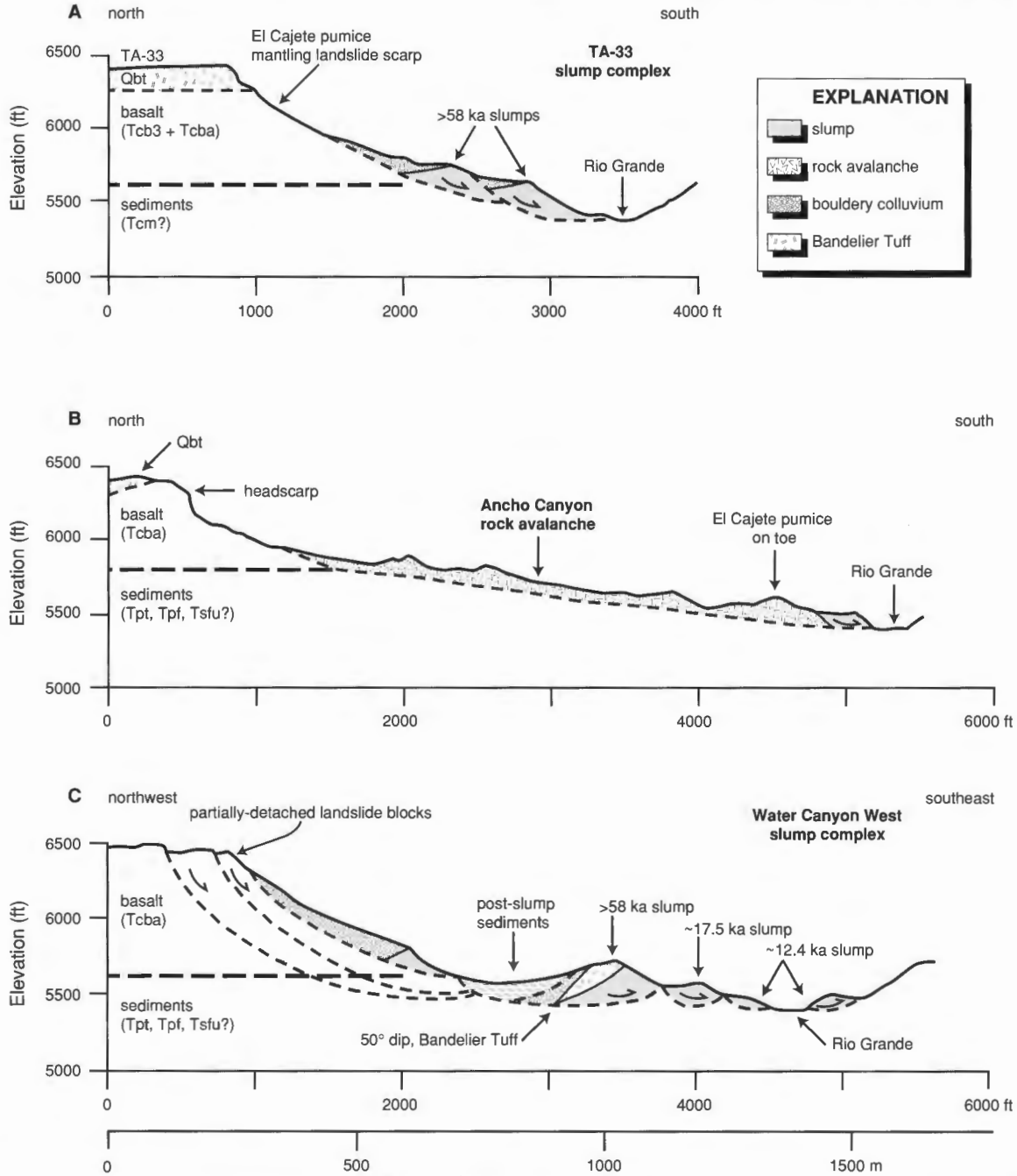

Fig. 12. Cross sections of landslides. (A) TA-33 slump complex. (B) Ancho Canyon rock avalanche. (C) Water Canyon West slump complex. See text and Plate 1 for description of bedrock units.

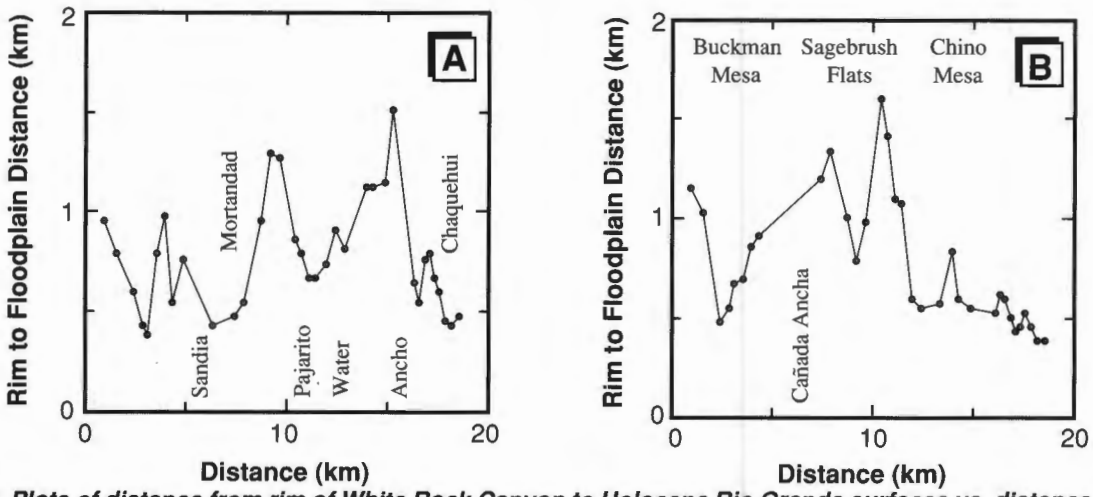

Fig. 13. Plots of distance from rim of White Rock Canyon to Holocene Rio Grande surfaces vs. distance downstream from Otowi bridge. (A) Northwest side of canyon. (B) Southeast side of canyon.

toes are eventually removed by erosion. The intervening areas with significantly higher slope gradient, such as the Overlook area (Fig. 14a), may be most susceptible to future failure, presuming that other factors are comparable (e.g., groundwater flow and rock strength).

The lower parts of failure planes are typically concealed beneath landslide debris in northern White Rock Canyon, preventing direct observation of the failure surface. Dips of planes between slump blocks near the canyon rim are 70 to 85°, but slope morphology, tilting of bedrock stratigraphy, and mechanical considerations suggest that deeper parts of those planes must have shallower dips (Figs. 12a and 12c). In general, massive failures appear to have occurred primarily along (1) steeply dipping planes rooted in the Santa Fe Group; (2) 10 to 30° planes (where measured) within the Puye Formation fanglomerate facies (Fig. 2b); and (3) subhorizontal planes in clayey silt layers found at several levels within Pliocene fluvial and lacustrine deposits.

Colluvial material covers rocks of the Santa Fe Group, the Puye Formation, or landslide deposits at most sites. El Cajete pumice lies on landslide deposits in areas south of Chaquehui Canyon, where fall deposits were thickest, indicating ages of >58 ka. The pumice occurs as isolated deposits on most landslides and on many colluvial slopes north of Chaquehui Canyon, but is apparently not present on others. Fluvial reworking of the El Cajete pumice makes geologic evidence for the age of pumiceous deposits equivocal at many sites. Soils on landslide deposits are generally 0.8 to 1.4 m thick. Carbonate morphology (Birkeland, 1984; Machette, 1985) is Stage IV at some sites, and Stage III carbonate is present in most exposures away from modern channels. By comparison with soils developed on terraces upriver along the Rio Chama (Dethier et al., 1988; Dethier and McCoy, 1993), Stage III and IV carbonate suggest ages of at least tens of thousands of years and perhaps in part greater than 100 to 200 ka for many of the landslides; however, because of differences in parent material between the landslides and the river terraces, these age constraints are not precise. Cation ratios in rock varnish (Dethier et al., 1988) on clasts from massive slumps at the southwest edge of La Mesita (Buckman Mesa) and in the Mortandad Canyon and Overlook zones (Fig. 11) suggest that those slides stabilized by at least 250 ka, although the accuracy of the varnish ages is uncertain. Contact relations with lacustrine deposits, discussed in a later section, provide additional age control.

Rock Avalanches

Two landslide deposits composed primarily of disaggregated basalt boulders along the northwest side of White Rock Canyon, near Ancho and Pajarito Canyons (Fig. 11), display surface features such as lateral ridges that indicate rapid, flowing motion of the rock debris. Geomorphic characteristics of these deposits are consistent with origins as long-runout rock avalanches (e.g., Hsu, 1975; Nicoletti and Sorriso-Valvo, 1991) from the western rim of White Rock Canyon. Long-runout avalanches travel significantly farther than predicted by normal frictional sliding, and this long runout is referred to as excessive travel distance. One mechanism that can account for the excessive distance is the generation of high dispersive forces associated with granular interactions within the basal slide layer (e.g., Hsu, 1975; Campbell, 1989).

The largest rock avalanche, which is north of the mouth of Ancho Canyon (Fig. 12b), has a surface area of about 0.50 km^2; using 20 to 40 m as a minimum average thickness provides an apparent volume of 10 to 20 x 10^6 m^3. The morphology at the avalanche head suggests that the original failure was about 350 m wide at the headscarp and that the failure included both intact rim and older landslide debris. Assuming that the avalanche originated near the present rim, it fell more than 300 m vertically and traveled about 1.5 km laterally to the Rio Grande, representing an excessive travel distance of about 1.0 km. Field mapping (Plate 1) suggests that the rock avalanche covers an older slide complex, but colluvium and talus obscure contacts. El Cajete pumice covers the upper slopes and toe areas of the slide, indicating that, despite its fresh appearance, it is older than 58 ka.

The rock avalanche deposit located along the northern margin of the Pajarito zone (Fig. 11) was not studied in detail, but superficially it resembles the much larger deposit at Ancho Canyon. The Pajarito rock avalanche fell about 200 m vertically and traveled about 1.0 km horizontally, for an excessive travel distance of about 0.68 km. The ratio of excessive length to total length for both rock avalanches (between 0.65 and 0.7) is typical for other long-runout avalanches described worldwide (Nicoletti and Sorriso-Valvo, 1991).

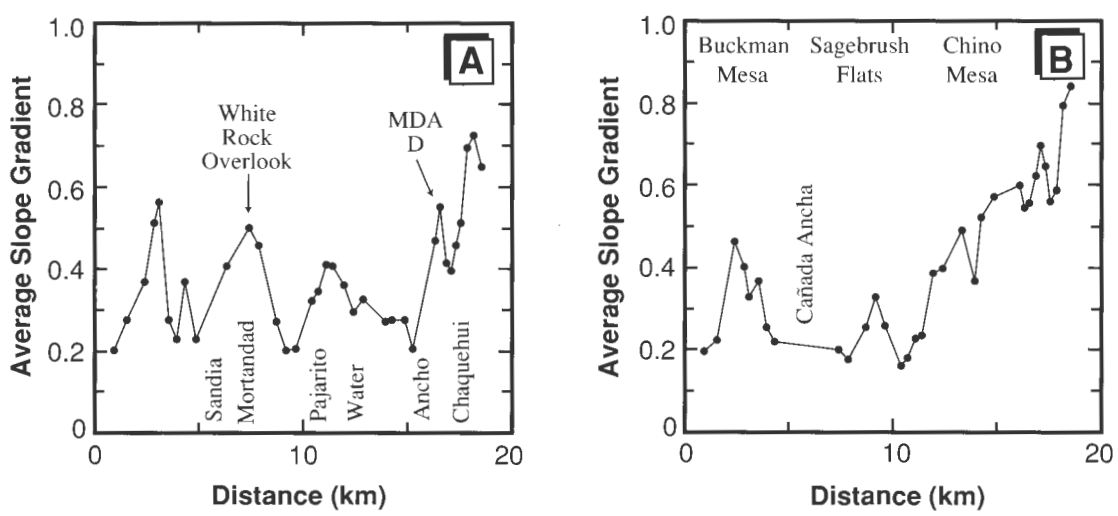

Fig. 14. Plots of average slope gradient in White Rock Canyon, defined as canyon depth divided by rim to floodplain distance (Fig. 13), vs. distance downstream from Otowi bridge. (A) Northwest side of canyon. (B) Southeast side of canyon.

Field evidence suggests that the Ancho Canyon rock avalanche may either have originated as a massive rock fall from a cliff or as a slide that rapidly disaggregated. The basaltic andesite of which it is composed is highly fractured and platy, and two scarps near the rim (Plate 1) suggest the potential for additional failures to the northeast. Sudden acceleration of the rock mass, produced by an earthquake on a nearby fault, is a plausible trigger for this rock avalanche, but failure could also have been related to the gradual decrease in stability of the slopes caused by long-term incision of White Rock Canyon and the removal of lateral support by previous landslides.

Translational Landslides

Probable translational landslides, where movement of relatively intact rock masses occurred along steep planar failure surfaces, have been observed in several areas in White Rock Canyon. These landslides are much smaller than the slumps and appear to occur predominantly in areas of thick basalt or Bandelier Tuff that may or may not overlie sedimentary rocks. One probable translational slide, extending about 50 to 100 m laterally along the slope, occurs in basalt east of MDA-D above lower Ancho Canyon. A second probable translational slide involving the exceptionally thick section of tuff that fills the early Quaternary paleocanyon (Fig. 5b) occurs in Chaquehui Canyon southeast of MDA-E.

Extensive movement of such translational slides may result in disaggregation, leading to rockfalls or debris flows. For example, four small mass-movement deposits, probably debris flows, consisting exclusively of Bandelier Tuff clasts occur in Chaquehui Canyon down canyon of MDA-E. The deposits rest on alluvial sediments of Chaquehui Canyon near the modern channel elevation and do not seem to be covered with El Cajete pumice; thus they are possibly late Pleistocene in age. These deposits may be part of debris aprons shed from adjacent cliffs of Bandelier Tuff, but may also be remnants of a larger landslide mass that flowed from upstream. Neither the slide material nor the stratigraphic context is similar to that of other slides examined in the area, and the deposits appear to be related to failure of the exceptionally thick tuff filling the early Quaternary paleocanyon.

Rockfalls

Rockfalls near TA-33 are characterized by the dislodgment of fracture-bounded blocks of bedrock and may constitute the primary form of mass wasting along many cliffs of basalt and Bandelier Tuff bordering White Rock Canyon and the tributary canyons. In this study, rockfalls were examined in detail only along the Bandelier Tuff cliffs that form the northeast rim of Chaquehui Canyon and the south-facing portion of TA-33 along White Rock Canyon. Cliff exposures included both unit 2 and unit 3 of the Tshirege Member.

In the detailed rockfall survey, the location of all young (latest Holocene) rockfalls of significant size that contained two or more blocks were recorded along 6.9 km of canyon rim (Plate 1). Rockfalls were judged to be young and of significant size when they met the following criteria: (1) one edge of each fallen block was greater than 50 cm; (2) the fallen blocks were generally unstable; (3) there was an absence of lichen cover, rock varnish, or weathering patina on fresh surfaces exposed by the rockfall; (4) caliche ($CaCO_3$) was present on most joint surfaces exposed by rockfall; and (5) there was no rounding of fresh surfaces of fallen blocks. The size characteristics of 23 areas where rockfalls had occurred were examined, and areas of widened joints, fresh fractures, and other evidence of incipient failure along the canyon rims were noted.

The mapped rockfalls all occurred in a zone within 3 m of the mesa rim and most involved a characteristic failure width of

less than 2 m and included less than five fracture-bounded blocks. One of the largest failures, which is on the mesa rim south of MDA-E, appears to have resulted from grading activities at the site. Grading and drainage diversion may also have contributed to some of the small rockfalls 50 m south of MDA-D. Evidence of incipient failure surfaces is also minimal. Two zones were found, neither near MDAs, where intersecting fracture sets outlined areas of potential failure between 3 and 4 m wide. If the assumption is made that all mapped rockfalls occurred randomly over the past 100 years, there is less than 50% chance of a rockfall occurring from any one kilometer of rim during a 10-year period. Rockfall events may not be random, but the characteristic failures are sufficiently small to prevent impact to the MDAs over short time periods.

Gullies

Small-scale gullies incised into late Pleistocene and Holocene sediments occur at many sites near TA-33. Gullies that were incised 40 cm or more in the vicinity of the mesa edges at TA-33 and near MDA-K were mapped and are shown on Plate 1. Active gullies are widely separated along most of the rim area. Two of the deepest gullies are cut into the Tshirege Member of the Bandelier Tuff by water diverted from roads near MDA-E and MDA-D. Neither gully represents a threat to these disposal areas. The gully system on the upland east of MDA-K is more extensive. Gullies near MDA-K are actively dissecting Quaternary deposits that include the >58 ka El Cajete pumice, and in many areas these deposits have been completely eroded to bedrock. Headward erosion of these gullies does not appear to represent a long-term threat to MDA-K because the erosion is largely restricted to the surficial deposits and is not incising the tuff. However, because of the widespread evidence for surface erosion near MDA-K, future transport of contaminated sediment down gradient from the outfalls is likely.

LANDSLIDE-DAMMED LAKES

Landslides blocked the Rio Grande in northern White Rock Canyon repeatedly during the late Pleistocene, and lake deposits preserve a record of the timing of these landslides as well as the location and size of the lakes. Lacustrine silt, clay and sand accumulated at elevations at least as high as about 5620 ft, about 60 m (200 ft) above the present level of the Rio Grande. The sites noted on Fig. 15 are the most extensive exposures of lacustrine sediment found to date. Stratigraphic relations and radiocarbon age control provide evidence for at least five separate lakes, and thus separate episodes of significant, presumably rapid, landslide movement. The age and inferred elevations of these lakes are shown schematically in Fig. 16 and are discussed in more detail below. The landslides that impounded these lakes occurred near the mouth of Water Canyon and may represent successive failures of the Water Canyon West slump complex (Figs. 10b, 11, and 12c). Reconnaissance field mapping suggests that slumps may also have dammed the Rio Grande in late Pleistocene time in the Pajarito Canyon zone (Figs. 10a and 11), perhaps at heights of a few tens of meters above the modern Rio Grande. Lake deposits conclusively tied to this landslide have not yet been found. It seems likely that the Rio Grande has been episodically dammed in White Rock Canyon by landslides at other times, although the evidence for these may have been largely obscured by subsequent landslides or removed by erosion.

Oldest Lake (≥ 43 ka)

Deposits of the earliest recognized lake are well exposed at the mouth of Cañada Ancha, near the Buckman townsite (Fig. 15), and provide evidence for the style of sedimentation in the landslide-dammed lakes of northern White Rock Canyon. Lacustrine sediment at the Buckman site (Figs. 17 and 18a) is exposed over a lateral distance of almost

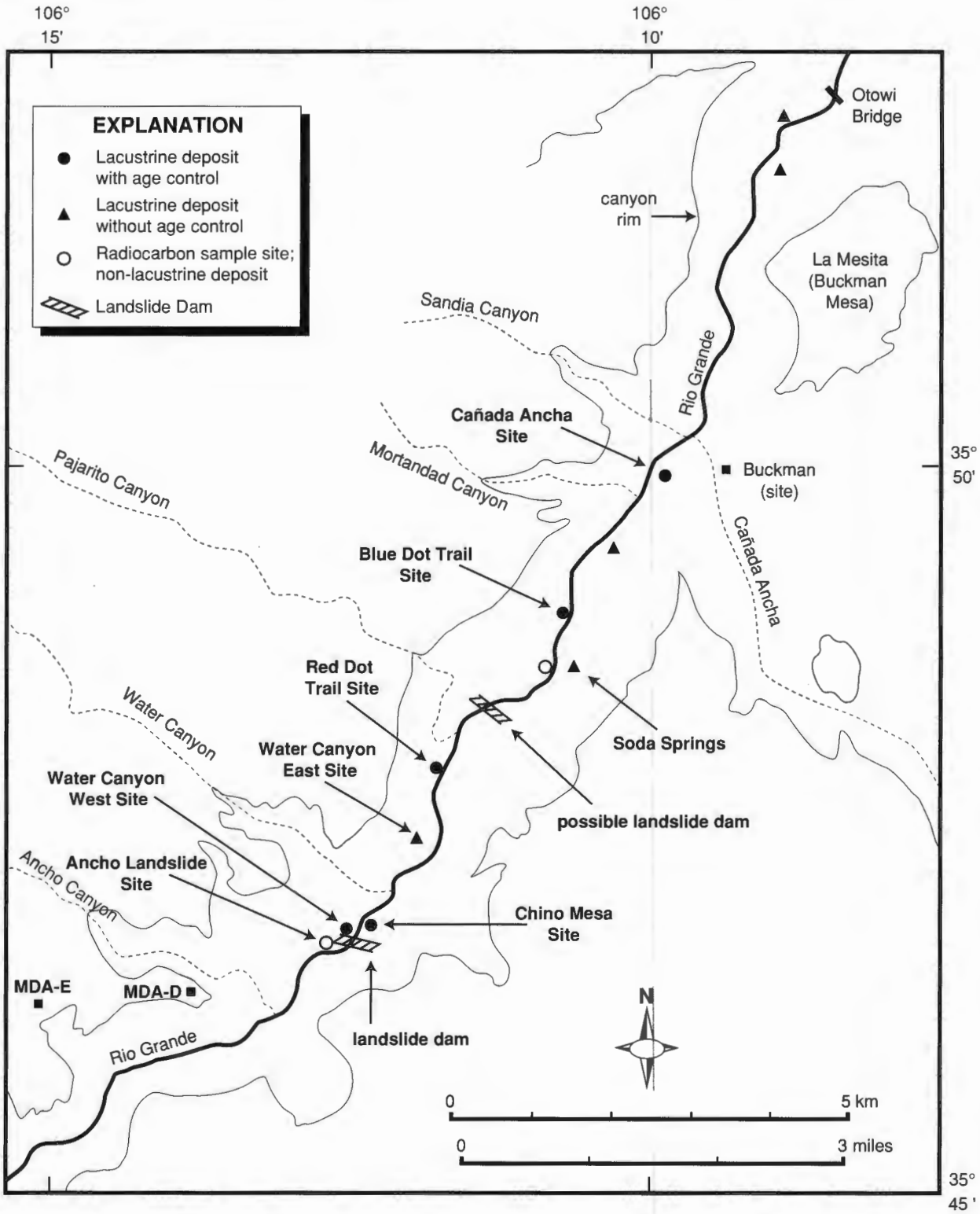

Fig. 15. Map showing location of lacustrine deposits, probable landslide dams, and radiocarbon dated sites in northern White Rock Canyon.

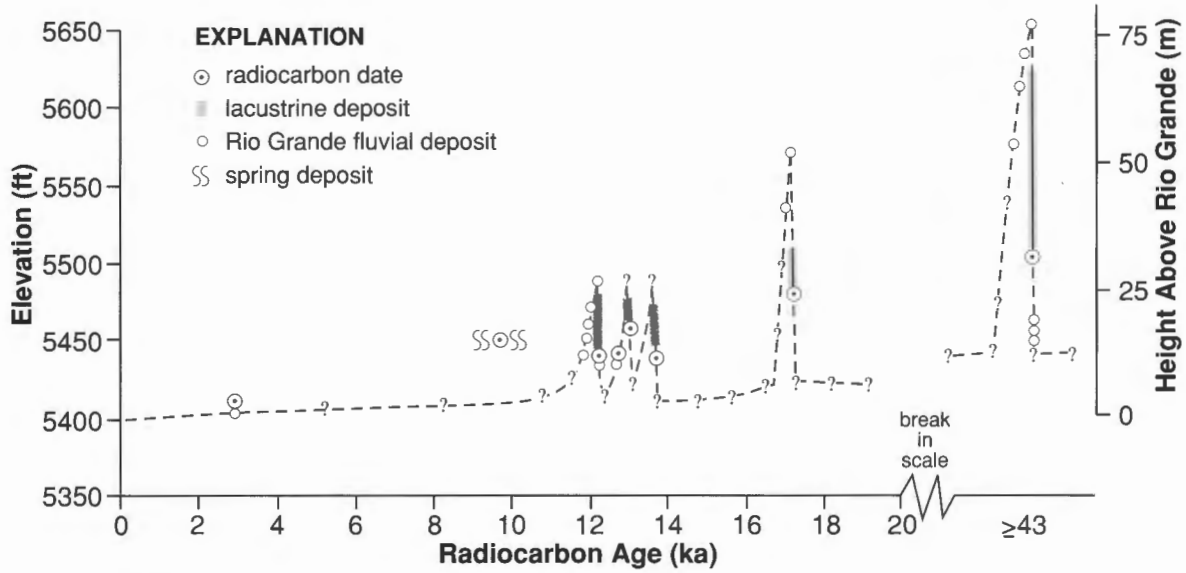

Fig. 16

Fig. 16. Diagram showing inferred water level in the Chino Mesa/Water Canyon West area. Data for sites other than Chino Mesa and Water Canyon West areas are plotted using elevation for lake deposits and height above the modern Rio Grande for river deposits and spring deposits.

200 m and extends 30 m vertically. The lower 15 m of sediment is rich in silt and clay and was deposited by turbidity flows in a lacustrine environment. The upper part of the section, above an unconformity, is sandier. The unconformable contact suggests that strong bottom currents within the lake eroded the silty deposits, although there is a slight possibility that the lake temporarily lowered and that the silts were subaerially eroded. The deposits near Cañada Ancha were previously noted by Griggs (1964) and interpreted as varved lake sediments by Galusha and Blick (1971), who related them to glacial activity in White Rock Canyon; however, there is no evidence for glacial activity at such low elevations.

Charcoal fragments collected from the base of the silt-rich sequence at Cañada Ancha have yielded an apparently finite AMS radiocarbon date of about 43.2 ka (WR-17, Table 3). Because this date is very close to the limit of radiocarbon dating and small amounts of contamination with modern carbon would erroneously provide a finite age, we consider the age of this deposit to be ≥43 ka. An additional age estimate is provided by comparing the elevation of the base of the lacustrine sequence at Cañada Ancha with dated fluvial deposits upriver. The basal sediments are only 15 to 20 m higher than the Rio Grande, a height associated with presumed middle or late Wisconsinan deposits (25 to 50 ka) north of White Rock Canyon along the Rio Chama (Q5 surface of Dethier and McCoy, 1993).

Possible correlative lacustrine sediments are located upriver near Otowi bridge and downriver near Soda Springs and Water Canyon. More than 20 m of similar fine-grained deposits are exposed southwest of Otowi bridge, on the west side of the Rio Grande (Fig. 15), although this outcrop has slumped and its original elevation is uncertain. Smaller exposures have also been mapped nearby on the east side of the river. High lacustrine sediments have been located as far downriver as the Water Canyon East slump complex, at an elevation of 5530 ft, and deposits of Rio Grande sands and cobbles in this area occur at up to 5650-ft elevation. These Rio Grande deposits may record the progradation of the river over lacustrine sediments as the lake filled, providing an estimate of the uppermost elevation of the lake, although they were not

TABLE 3
RADIOCARBON DATES FROM WHITE ROCK CANYON

Field Number	Laboratory Number *	14C Date (yr B.P.)_	δ13C (o/oo)	Calibrated Age** (cal BP)	Sample Site	Deposit
WR-12	Beta-64516	2,880 ± 80	***	2983 (2739-3447)	Soda Springs reach	floodplain; probable paleo-campsite
WR-16	Beta-67824, CAMS-9907	9,660 ± 60	-24.6	10,910 (10380-11010)	Blue Dot Trail area	colluvium; probable spring deposit
WR-17	Beta-64518, CAMS-8283	43,200 ± 250#	-23.1	(too old for calibration)	Buckman area	basal lake sediments
WR-18	Beta-64519, CAMS-8284	17,450 ± 120	-22.9	20,760 (20370-21120)	Water Cyn W. area	buried soil
WR-20	Beta-64520, CAMS-8285	12,300 ± 50	-25.5	14,370 (14020-14780)	Red Dot Trail area	buried soil
WR-23	Beta-67825, CAMS-9908	13,650 ± 60	-24.2	16,360 (15990-16710)	Chino Mesa area	buried soil
WR-24	Beta-65158, CAMS-8334	15,070 ± 70	-24.4	17,990 (17650-18320)	Chino Mesa area	buried soil
WR-25	Beta-65159, CAMS-8335	12,380 ± 60	-24.8	14,480 (14080-14940)	Chino Mesa area	buried soil
WR-26	Beta-67826, CAMS-9909	13,070 ± 60	-23.6	15,550 (15060-15960)	Chino Mesa area	buried soil
WR-27	Beta-65160, CAMS-8336	12,370 ± 70	-23.4	14,460 (14030-14970)	Chino Mesa area	buried soil
WR-30	Beta-67827, CAMS-9910	12,800 ± 60	-25.4	15,110 14620-15560)	Ancho landslide area	Rio Grande sands
WR-31	Beta-67828, CAMS-9911	12,370 ± 70	-24.6	14,460 (14030-14970)	Red Dot Trail area	buried soil
WR-32	Beta-67829, CAMS-9912	12,430 ± 70	-27.0	14,550 (14100-15060)	Red Dot Trail area	basal lake sand
WR-34	Beta-67830, CAMS-9913	12,570 ± 70	-25.4	14,750 (14270-15270)	Chino Mesa area	buried soil
WR-35	Beta-67831, CAMS-9914	13,180 ± 60	-23.3	15,710 (15250-16110)	Chino Mesa area	basal lake sand

Notes:
* Laboratory designations: Beta = Beta Analytic Inc; CAMS = Lawerence Livermore National Laboratory AMS Facility.
** Calibrated ages use computer program CALIB 3.03 of Stuiver and Reimer (1993), with error multiplier of 2.0 and 2σ uncertainty. Ages in ( ) are 2σ range. For sample that was not corrected for δ13C in laboratory, the δ13C value was assumed to be -24.4 ± 1.1 o/oo based on δ13C values of 14 samples collected from White Rock Canyon.
*** Radiocarbon date was not corrected for δ13C.
# Considered to be minimum-limiting age because of small sample size and possibility of laboratory contamination.

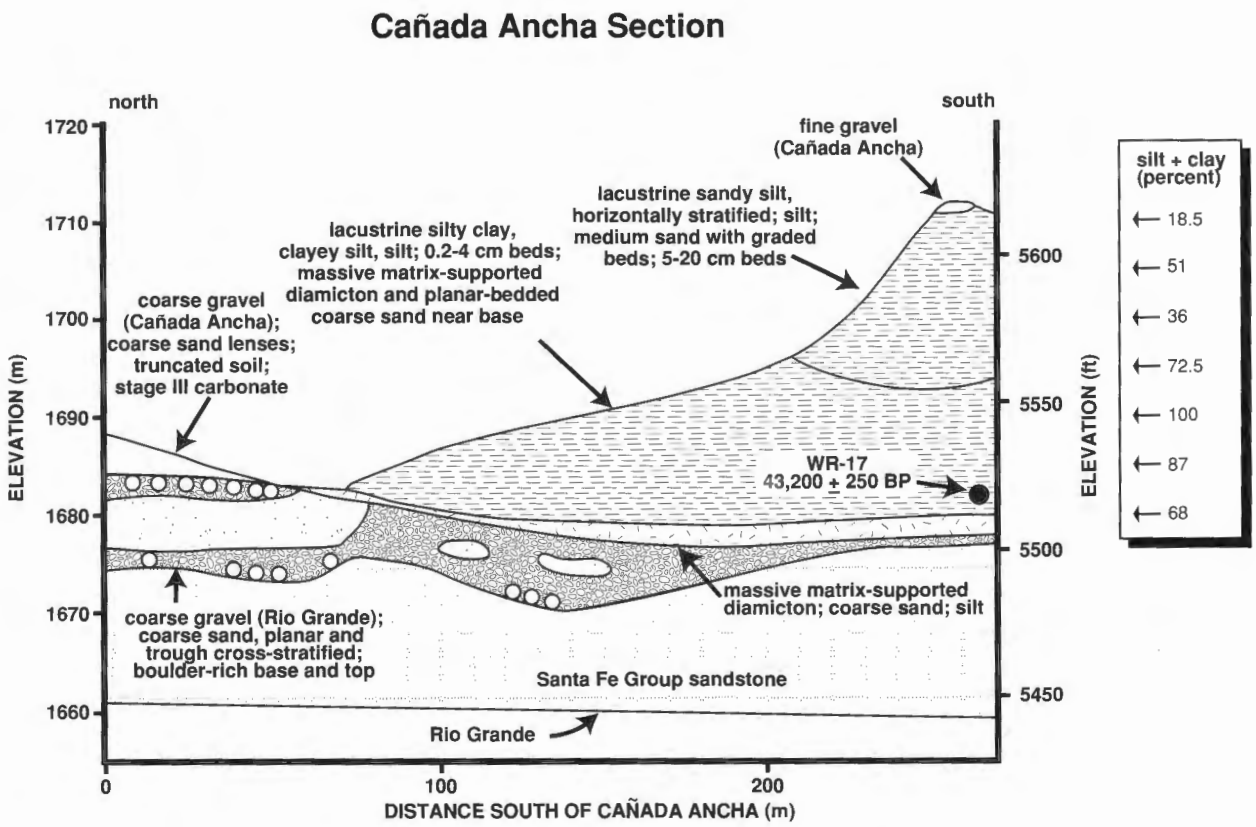

Fig. 17. Sketch of stratigraphic section exposed near the mouth of Cañada Ancha.

observed to rest directly on lacustrine sediments. Rio Grande terraces occur at similar elevations near Otowi bridge and above lower Sandia Canyon and may also record re-establishment of the river after filling of the lake. As the lake and river deposits downriver both overlie the upriver side of the Water Canyon East slump complex, it is possible that this landslide was responsible for damming the Rio Grande. The canyon is much narrower at the Water Canyon West slump complex, however, and the latter area may have been the actual dam site.

The dimensions of the lake can be estimated by making several assumptions about the location of the dam, the maximum elevation of the lake, and the height of the Rio Grande at that time. Here we assume that the dam was at the Water Canyon West slump complex, that the river at that time was 15 to 20 m above the modern channel, and that the maximum lake elevation is either recorded by the top of the Cañada Ancha lacustrine section (5620 ft) or by the highest Rio Grande deposits that may be associated with filling of the lake (5650 ft at Water Canyon East slump complex). Maximum lake depth is thus estimated at 48 to 62 m, with a corresponding length of about 24 to 33 km, extending to the vicinity of Española, although it is possible that the lake was actually larger or smaller than this. For example, if the dam was "leaky" or if the dam grew by continued landsliding as the lake filled, the lake may not have reached the outflow level until significant sedimentation had occurred, in which case the actual

Fig. 18. Photographs of laminated lacustrine sediments in White Rock Canyon. (A) Lower silt and clay rich sediments at Cañada Ancha site near WR-17 sample site; dated at ≥ 42.3 ka. (B) Lower fine sand and silt layers at Red Dot Trail area. Pocket knife is at basal coarse sand layer of lacustrine deposit overlying terrestrial sand deposit dated at 12.3 ka (WR-20).

lake dimensions would have been smaller. Alternatively, the high Rio Grande gravels may have slumped since deposition, resulting in an underestimation of lake size.

Intermediate Lake (≤ 17.5 ka)

Evidence for the next younger landslide-dammed lake is exposed at the east edge of the Water Canyon West slump complex. Lacustrine sediments occur up to 27 m above the modern channel (to an elevation of 5490 ft)on the upstream side of a landslide derived from the toe of the larger slump to the west (Figs. 19 and 20). Charcoal collected from a buried soil directly beneath these sediments yielded a ^{14}C age of 17.5 ka (WR-18, Table 3), providing a maximum-limiting age for the lake and the associated landslide. Above the outcrops of lacustrine sediment, 50 m above the modern channel at an elevation of 5535 ft, a levee composed of large basalt boulders lines an abandoned outlet channel for this lake over the landslide dam (Figs. 19 and 20). On this same landslide, boulder gravel containing Rio Grande lithologies occurs as high as 60 m above the modern channel to an elevation of 5570 ft, possibly recording the progradation of the Rio Grande after filling of the lake and providing an estimate of the maximum lake elevation. However, it is also possible that these high gravels are older, unrelated to this lake and involved in the landslide.

Deposits from this lake may also be present on the east side of the Rio Grande below Chino Mesa and may be involved in the younger landslide damming events that are discussed below. On the downstream side of the younger dam, exposed clayey lacustrine sediments are exposed that dip 25° to the west (Figs. 19 and 20), demonstrating transport as part of a landslide, although the age of these sediments has not been determined. On the upstream side of the dam, a radiocarbon date of 15.1 ka (WR-24, Figs. 19 and 21, Table 3) was obtained from charcoal fragments within a buried soil that overlies lacustrine sediments. If this age is accurate, the lacustrine deposits may be associated with the ≤17.5 ka lake and also involved in younger landsliding, although the context of these sediments is not certain. An alternative explanation is that these sediments record an additional lake that is >15.1 ka in age.

Youngest Lakes (≤13.7 ka to ≤12.4 ka)

Deposits of three younger lakes have been examined along a 6-km stretch of river extending upstream from the Water Canyon West slump complex, in particular sites near Chino Mesa and the Red Dot and Blue Dot trails (Fig. 18b). The Rio Grande was apparently dammed by repeated failures of the toe of this slump complex during a 1200- to 2600-year period in the latest Pleistocene (using calibrated ^{14}C ages; Tables 3 and 4), indicating an extensive period of instability. Age constraints are provided by radiocarbon dates on charcoal collected from buried soils overlying or underlying lacustrine sediments or Rio Grande deposits and from coarse basal sands beneath lacustrine sediments. The coarse basal sands are believed to represent transgressive beach deposits produced as the lake levels rose, although they may possibly record pulses of sediment from local arroyos.

Two episodes of lake-level rise after about 13.7 ka and before 12.4 ka are recorded at the Chino Mesa site (Fig. 19) by a repeating sequence of lacustrine sands, silts, and clays between 14 and 22 to 24 m above the modern Rio Grande, overlain by dark, organic-rich buried soils (Fig. 21). The exact chronology of these lakes is not certain because of some inconsistency between ^{14}C dates (e.g., an age of 13.2 ka [WR-35] was obtained from basal sand that overlay a buried soil with a younger age of 12.6 ka [WR-34]), but the stratigraphy and age control suggest an intervening period of terrestrial exposure that terminated around

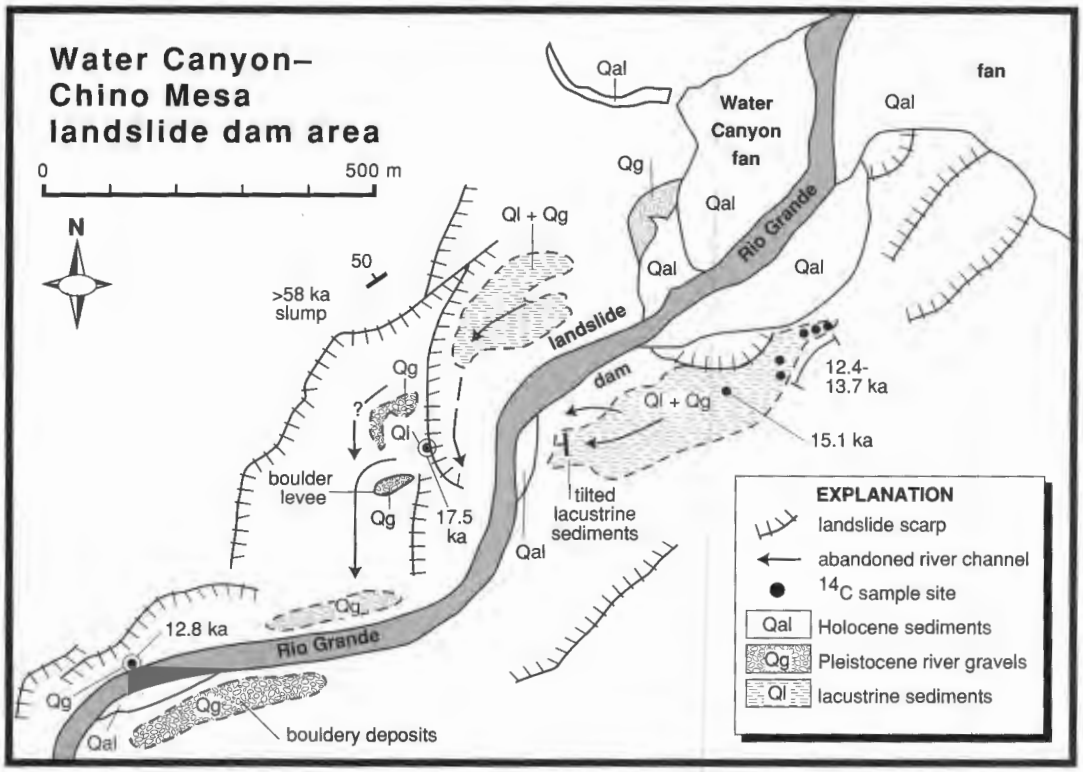

Fig. 19. Sketch map of Water Canyon West-Chino Mesa landslide dam area.

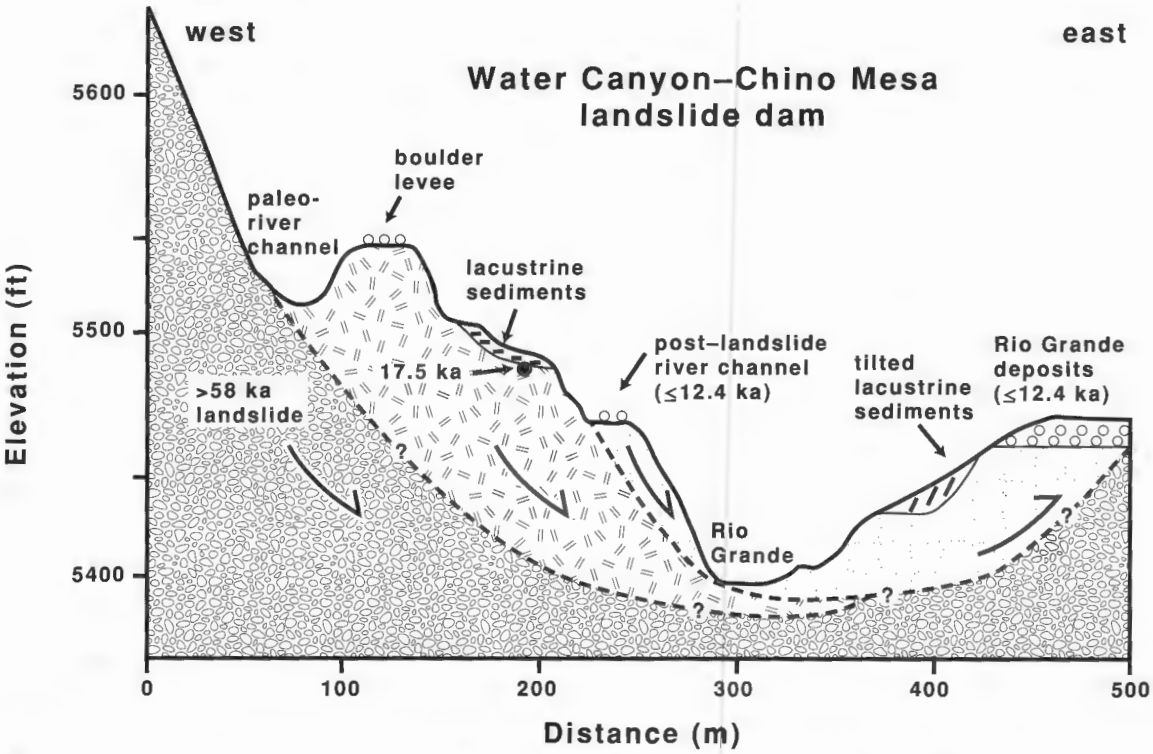

Fig. 20. Schematic cross-section through Water Canyon West-Chino Mesa landslide dam area.

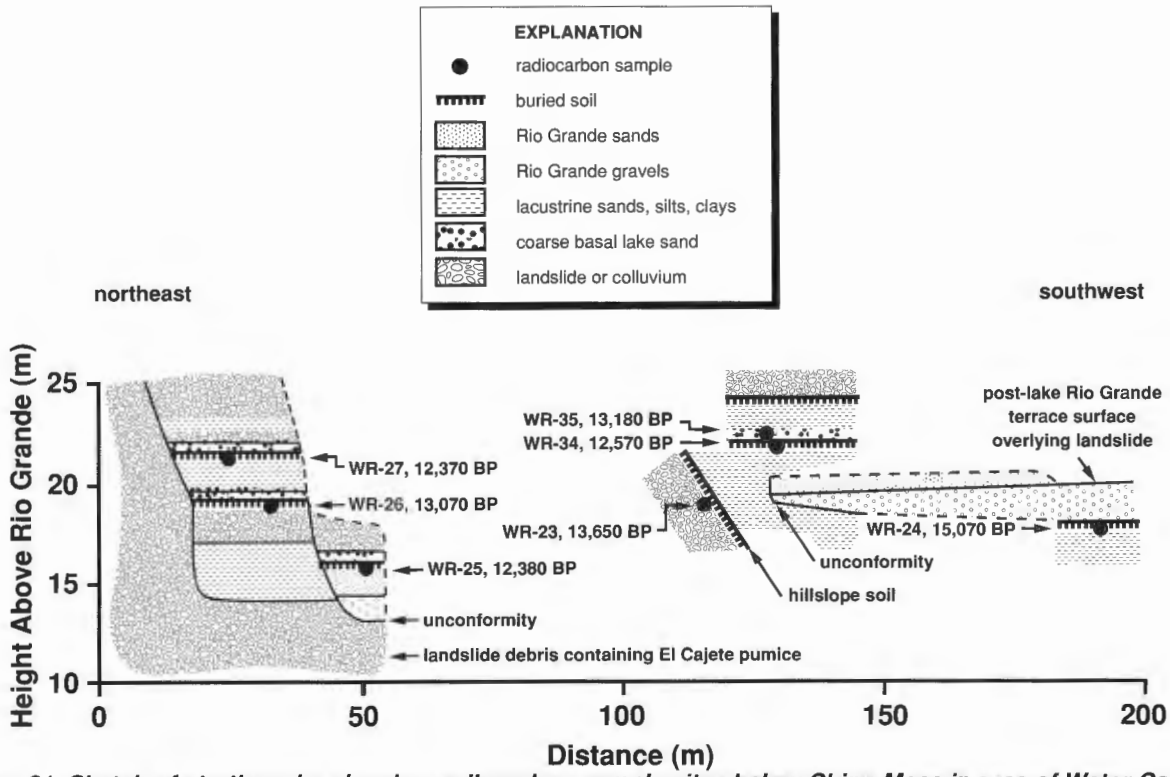

Fig. 21. Sketch of stratigraphy showing radiocarbon sample sites below Chino Mesa in area of Water Canyon West dam.

13.1 ka (WR-26 and WR-35, Table 4). It is possible that the lake never completely drained during this period, perhaps persisting with a fluctuating water level due to a "leaky" dam. It seems more likely from the stratigraphy, however, that two distinct lakes separated by several hundred years are recorded in the deposits. Before about 12.4 ka (WR-25), the Rio Grande flowed through the landslide dam, depositing fluvial sediments as low as 13 m above the modern channel that were inset into the older lacustrine sediments (Fig. 21). Charcoal collected from possible correlative Rio Grande deposits 13 m above the river downstream of the dam has yielded a ^{14}C date of ca. 12.8 ka (WR-30, Fig. 19, Table 3), suggesting that the second lake had drained by that time.

A third lake in the latest Pleistocene is well constrained by deposits at both the Chino Mesa and Red Dot sites. Five statistically indistinguishable radiocarbon dates of 12.3

TABLE 4
AVERAGED RADIOCARBON AGES FROM WHITE ROCK CANYON

Geologic Unit	Averaged 14-C Age (yr B.P.)*	Calibrated Age (CALIB 3.03)**	Samples
youngest lake	12,364 ± 74	14,460 cal BP (14,830-14,140)	WR-20, WR-25, WR-27, WR-31, WR-32
intermediate lake	13,126 ± 99	15,630 cal BP (15,990-15,220)	WR-26, WR-35

Notes:
* Averaged radiocarbon ages were obtained using computer program CALIB 3.03 (Stuiver and Reimer, 1993) withan error multiplier of 2.0 for the original analyses. Average ages were obtained from samples from presumed correlative units where there is no statistically significant difference between sample ages.
**Calibrated ages use 2σ uncertainty, from Stuiver and Reimer (1993). Ages in ( ) are 2σ range.

to 12.5 ka have been obtained from buried soils or basal sands (Figs. 21 and 22; Tables 3 and 4), closely constraining the initiation of this lake and the most recent major landslide movement at the Water Canyon West slump complex. Characteristics of the buried soils suggest that relatively little time may have elapsed since termination of the previous lake, which is consistent with the available age control. The WR-20 (Fig. 18b) and WR-25 soils show no evidence for significant exposure time; terrestrial exposure is only shown by burrowed sands at both sites and by land snails (*Succinea*) in the WR-20 deposit. The WR-27 and WR-31 soils both have dark A horizons, indicating accumulation of organic matter, but this may also have required little time in a moist environment.

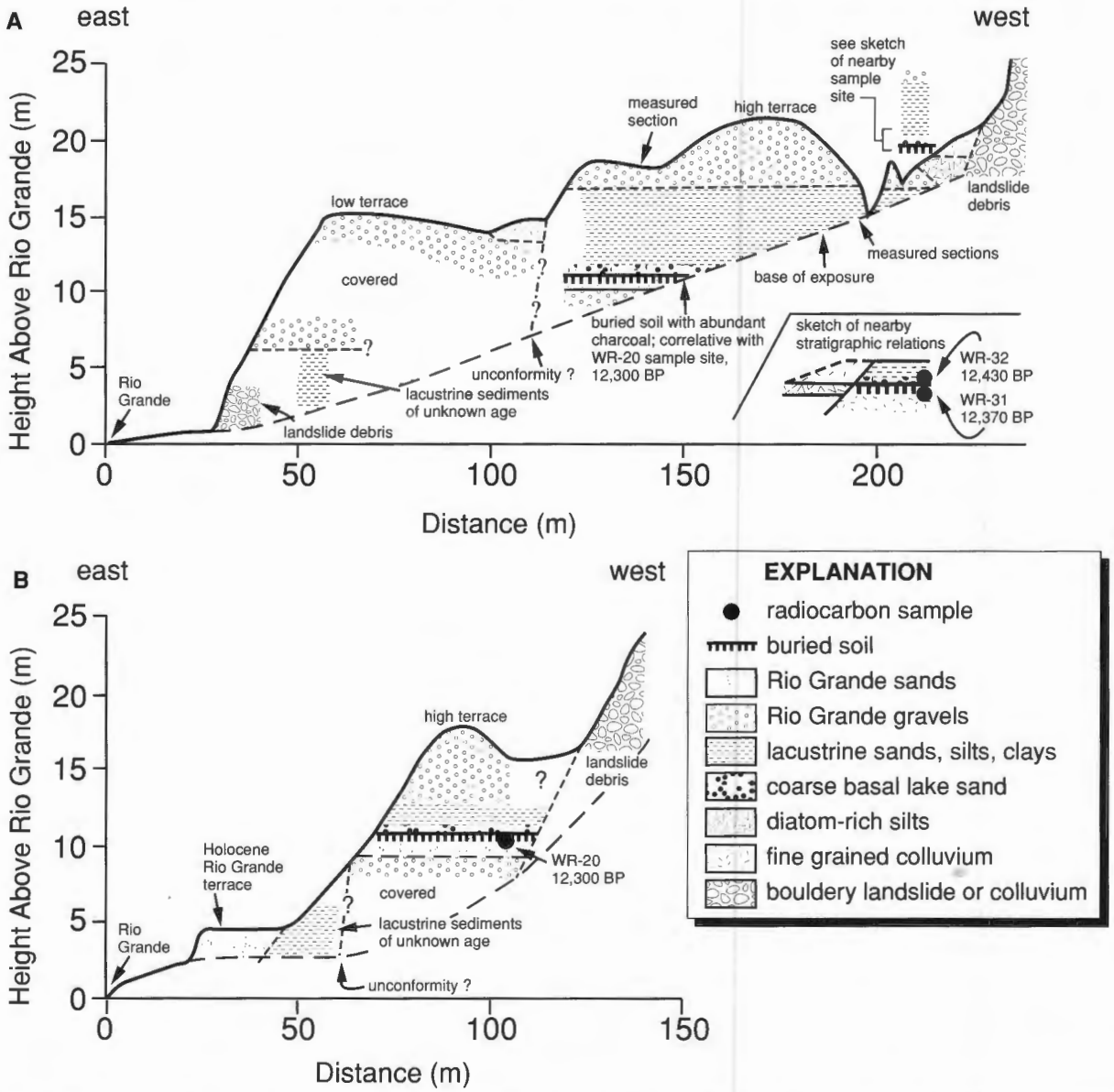

Fig. 22. Cross-sections of Red Dot Trail area showing stratigraphy and radiocarbon sample sites. (A) Northern section, site of measured stratigraphic sections in Fig. 24. Inset shows stratigraphic relations at nearby WR-31 and WR-32 sample sites 30 m south of section. (B) Southern section, 150 m south of (A), showing WR-20 sample site.

The upper limit of the lake at the Red Dot site is suggested by lacustrine sediments and possibly associated river gravels about 24 m above the modern channel (~5485-ft elevation). Following re-establishment of the Rio Grande at the Red Dot site, the channel incised and temporarily stabilized at heights of about 17 to 21 m and later at 6 to 15 m, as recorded by inset river terraces (Fig. 22). The lower of these river terraces at the Red Dot site is underlain by an additional sequence of lacustrine sediments that extends to within 4 m or less of the modern channel (Fig. 22), although the age and context of these sediments are not known. The 12.4 ka lake is estimated to have extended upriver to near Otowi bridge, with a maximum lake depth of 15 to 27 m and a possible length of 14 km.

Deposits in the Blue Dot Trail area are similar to those at the Red Dot Trail site, including two Rio Grande terraces developed above lacustrine sands that in turn overlie Rio Grande gravels (Fig. 23). The Blue Dot deposits are presumed to record the ≤12.4 ka lake because of their similarity in character and elevation to the Red Dot deposits, although precise age control has not been obtained here. The only age constraint is a minimum-limiting age of 9.7 ka (WR-16) obtained from possible spring deposits behind the higher river deposits (Fig. 23). The Rio Grande flowed within several m of its present elevation by at least 2.9 ka, which is shown by a radiocarbon date obtained from deposits near the present river near Soda Springs (WR-12, Table 3).

At both the Red Dot and Blue Dot sites, thin-bedded, silt-rich fine sand is the most common lacustrine sediment (Figs. 18b, 24, and 25). Cross-laminated to cross-stratified beds suggest that moderate to strong currents swept the bottom of the lake or lakes at irregular intervals, perhaps when nearby arroyos were in flood. Neither the Blue Dot nor the Red Dot sections expose other evidence for breaks in sedimentation.

Effects of Lake Drainage

Termination of some of the landslide-dammed lakes in White Rock Canyon may have resulted in significant secondary effects such as catastrophic downstream flooding or the triggering of additional landslides. The strongest evidence for such effects of lake drainage are boulder-rich deposits that extend for at least 12 km below the Water Canyon West dams. These deposits have only been examined in reconnaissance.

Remnants of alluvial surfaces underlain by deposits rich in large basalt boulders occur for at least 3 km downstream from the Water Canyon West dam. These boulders are up to several meters in diameter and are locally polished or imbricated. The alluvial surfaces apparently decrease in height above the river from about 23 m near the dam to about 9 m near Chaquehui Canyon, with a gradient of about 0.004 that is significantly steeper than the modern river gradient of about 0.002. The steep gradient and the abundance of basalt boulders suggest deposition from an extreme flood event, such as would be associated with drainage of a landslide-dammed lake. Alternatively, the basaltic debris may have been derived from the relatively slow erosion of the dam, although a catastrophic failure seems more likely. These deposits start at the downstream end of the Water Canyon West dam, suggesting an age between about 17.5 and 12 ka.

Similar boulder-rich deposits located significantly higher above the Rio Grande have been mapped 8 to 12 km downstream of the Water Canyon West dam in the Cochiti Dam quadrangle, between Frijoles and Alamo Canyons. The surfaces of these deposits have an apparently steeper gradient of about 0.006. Near the mouth of Lummis Canyon, the deposits contain boulders as large as 4 m (b-axis) and are overlain by the El Cajete pumice, indicating an age of

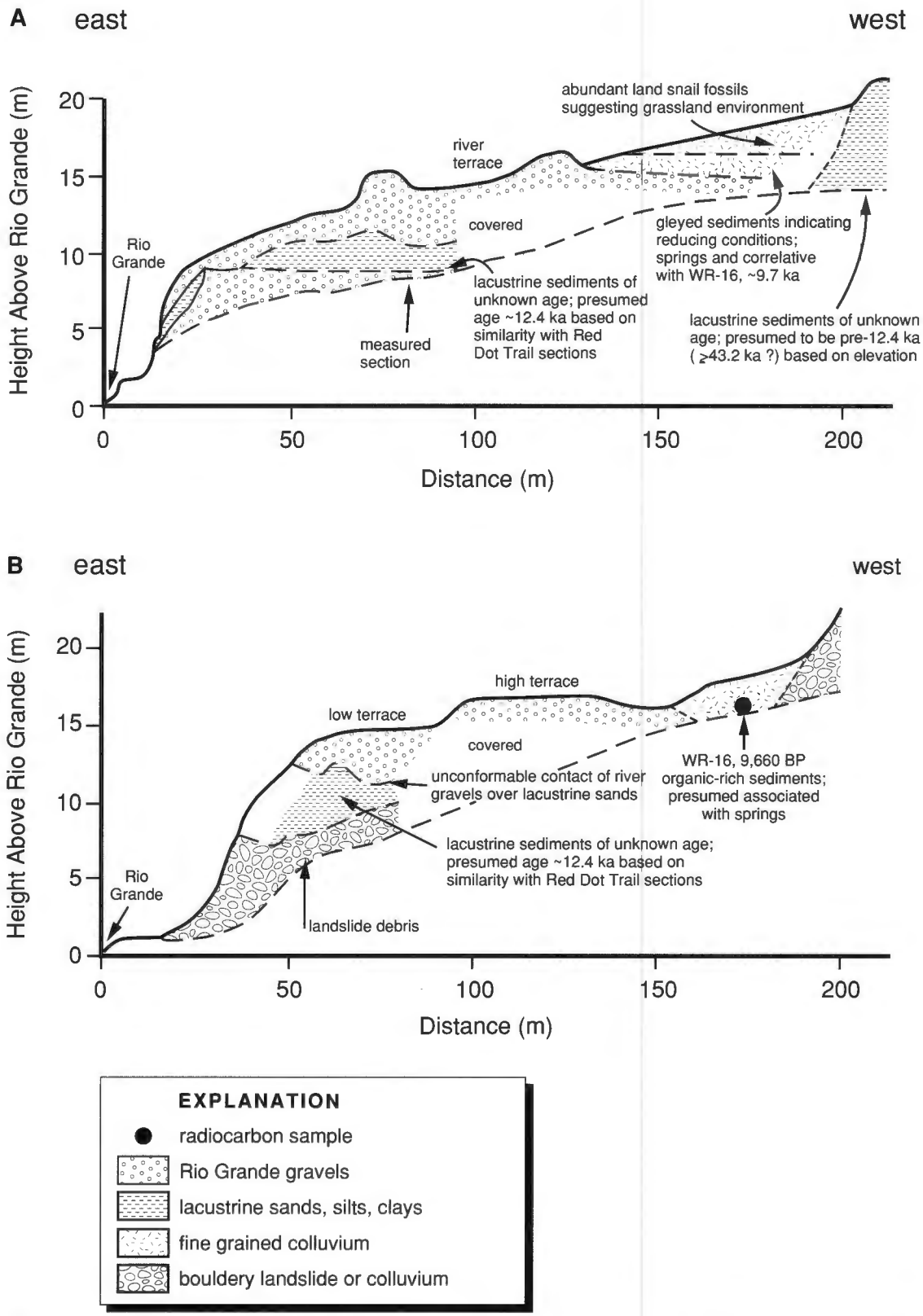

Fig. 23. Cross-sections of Blue Dot Trail area showing stratigraphy and radiocarbon sample sites. (A) Northern section; site of measured stratigraphic section in Fig. 25. (B) Southern section 130 m south of (A) showing WR-16 sample site.

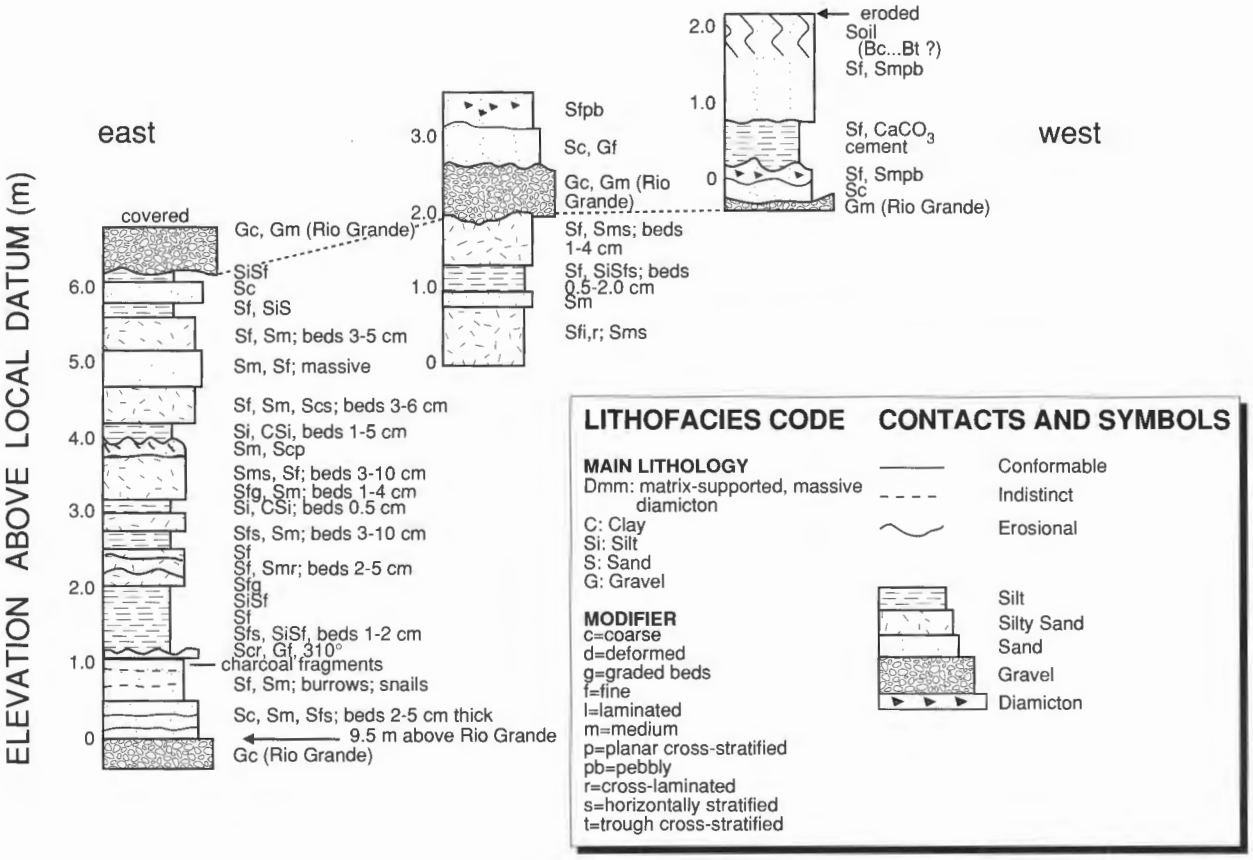

Fig. 24. Measured stratigraphic sections exposed in the Red Dot Trail area.

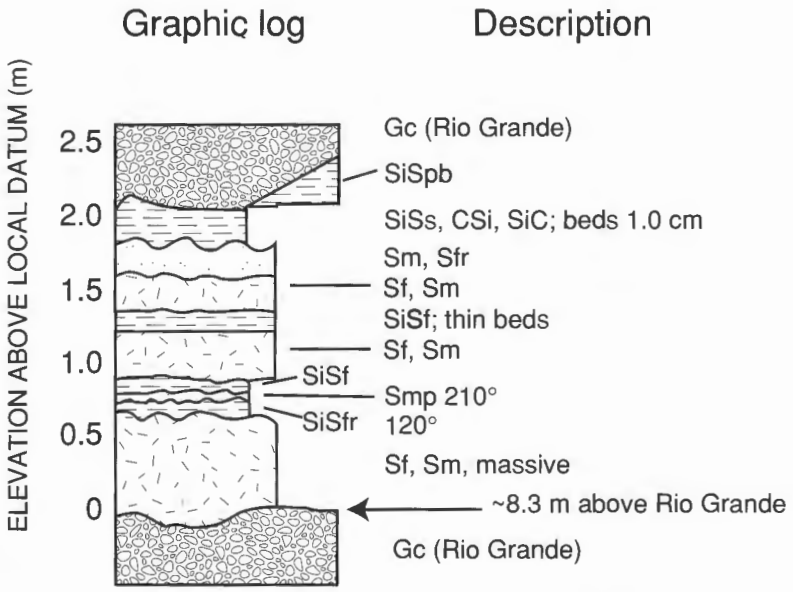

Fig. 25. Measured stratigraphic section exposed near the Blue Dot Trail area. See Fig. 24 for explanation of symbols and lithofacies codes.

greater than 58 ka. It is possible that they were produced by erosion and deposition from an earlier catastrophic flood that results from rapid lake drainage, although these deposits cannot at present be related to any specific lake.

Extensive downstream bank scour and possible triggering of additional landslides may have accompanied lake-draining floods in White Rock Canyon, but because the landslide dam is located near the downstream extent of the large slump landslides, the effect of such floods on landslides may have been minor. An additional potential effect of sudden draining of lakes is the triggering of landslides within the area of the lake, which could have been caused by high seepage pressures in the banks, analogous to well-documented cases of landslides triggered by the rapid drawdown of reservoirs (e.g., Selby, 1982). Some of the landslides occurring upstream of the Water Canyon West slump complex may have been triggered or reactivated as lakes drained, although data on the timing of such landslides have not been obtained.

Causal Factors

The ages of the latest Pleistocene lakes in White Rock Canyon correspond to a period of global climate changes associated with the peak and termination of the most recent major glaciation in North America (the late Wisconsinan glaciation) and thus suggest a direct relation between these climate changes and triggering of the landslides. The upper Rio Grande drainage in New Mexico and Colorado supported extensive alpine glaciers during the late Pleistocene, and evidence from elsewhere in the Rocky Mountains indicates that the peak of late Pleistocene glaciation occurred about 22 ka, and that these glaciers had largely disappeared by 10 to 12 ka (e.g., Porter et al., 1983; Richmond, 1986). At least two connections between these climate changes and slope stability in White Rock Canyon are reasonable.

First, varied evidence indicates that precipitation in the region was significantly higher during the latest Pleistocene than at present. Increased precipitation would have resulted in higher recharge rates to the aquifer beneath the Pajarito Plateau, in turn producing higher water table elevations and higher groundwater discharge rates in White Rock Canyon, thus decreasing the stability of the slopes, although the precise difference in precipitation has been difficult to quantify. Studies of the Estancia basin in central New Mexico show that separate highstands of Pleistocene Lake Estancia occurred between roughly 20 and 15 ka and later between 14 and 12 ka (Bachhuber, 1989; Allen, 1991; Allen and Anderson, 1993). Allen and Anderson (1993) argue that these high lake levels must record regional precipitation significantly higher than at present, and they also infer that groundwater discharge in the Estancia basin decreased significantly after about 12 ka. Studies of Pleistocene Lake San Agustin in central New Mexico also suggest that between 14 and 27 ka there was significantly higher stream flow than today, and that there were also major climatic fluctuations during this period (Phillips et al., 1992). Similarly, Phillips et al. (1986) used isotope data from groundwater in the San Juan Basin of northwest New Mexico to infer that groundwater recharge during the late Pleistocene was significantly higher than at present. The paleobotanical record from the American southwest also supports higher regional precipitation during the period from 16 to 10 ka, derived primarily from winter storms; however, the magnitude of the inferred precipitation changes and their timing are not fully understood (e.g., Spaulding et al., 1983; Van Devender et al., 1987; Spaulding, 1992). It should be stressed, however, that there was undoubtedly a lag between periods of maximum recharge and maximum spring discharge, and therefore the period of minimum slope stability may not correspond to the period of maximum precipitation.

Second, peak flood discharges along the Rio Grande in the latest Pleistocene could have been significantly higher than at present because of the higher regional precipitation, the melting of glaciers, or other climatic changes such as warmer temperatures leading to rapid melting of snowpacks. Such high flood discharges could have triggered the toe failures by leading to rapid incision within White Rock Canyon or scouring of the toes of landslide complexes. At present, floods associated with snowmelt runoff have the longest duration and, typically, the highest annual peak discharge—up to 25,000 cfs at Otowi bridge since measurements began in 1895 (Graf, 1994). Higher peak discharges during parts of the Pleistocene with higher regional snowfall are thus reasonable, although no estimate of the magnitude of this difference has been made. Although the chronology of deglaciation in the southern Rocky Mountains is not well defined, available evidence suggests that the youngest White Rock Canyon landslide-dammed lakes, at ca. 13.7, 13.1, and 12.4 ka, may have been created during the period of major late-Wisconsin deglaciation in the Rocky Mountains (e.g., Porter et al., 1983; Richmond, 1986; Elias et al., 1991). This concurrence of ages in turn suggests that higher flood discharges related to glacial melt may have been a significant contributing factor to the landslides. Dethier and McCoy (1993) proposed that the Rio Chama underwent rapid incision sometime between deposition of their Q5 surface (>25 ka) and the Holocene (10 ka), and higher incision rates along the Rio Grande in White Rock Canyon during this time period may have contributed to the toe failures.

LONG-TERM EVOLUTION OF WHITE ROCK CANYON

An understanding of the long-term evolution of White Rock Canyon provides important insights for evaluating the relative susceptibility of different parts of the canyon to landsliding and the time scales of failure. Evidence pertaining to the long-term evolution of White Rock Canyon is provided by observations of spatial and temporal variations in landsliding, which is discussed in previous sections, and observations of differing characteristics of the early Quaternary canyon and the modern canyon.

White Rock Canyon downriver from TA-33, is incised largely into basalts and is much narrower than upriver (Fig. 7), where it is incised into both basalts and the underlying sediments. In addition, the 1.2-Ma paleocanyon of the Rio Grande exposed near TA-33 appears to differ significantly in morphology from the modern canyon. Available exposures indicate that the early Quaternary canyon was much shallower and narrower than the modern canyon (Fig. 7); it was incised largely into basalts and associated phreatomagmatic deposits and apparently lacked the extensive slump landslides that flank the modern canyon. These morphologic differences suggest that large-scale landslides only occur after canyon incision exposes a significant thickness of sedimentary rocks with much lower shear strength than the basalts. These observations also suggest that the style and rate of widening of the canyon may have varied significantly over time as the Rio Grande cut down through a variety of stratigraphic units.

We propose a simple model for the long-term evolution of White Rock Canyon, in which canyon widening by mass-wasting is initially slow through basalts and related rocks and then increases significantly with the exposure of weaker underlying sedimentary rocks and the initiation of massive slump landslides (Fig. 26). The time of initiation of the major landslides is not known, although it would have varied along the canyon in relation to the time of exposure of a sufficient thickness of sedimentary rocks beneath the basalts. The elevation of the lowermost basalts exposed along the canyon walls generally decreases downcanyon from Otowi bridge (Dethier, 1995), and landslides

would thus be initiated earlier upcanyon, assuming that the gradient of the Rio Grande has been roughly constant since the early to middle Pleistocene.

A series of simplifying assumptions need to be made in order to approximately quantify the timing of landslide initiation and the rates of canyon widening by landsliding. (1) Incision rates along the Rio Grande have been roughly constant for the last 500,000 to 700,000 years. (2) Sedimentary rocks beneath the basalts have uniform strength properties (friction angle, cohesion). (3) Groundwater discharge has been spatially and temporally uniform along the canyon walls. (4) Slumps can be initiated once a threshold thickness of sedimentary rocks

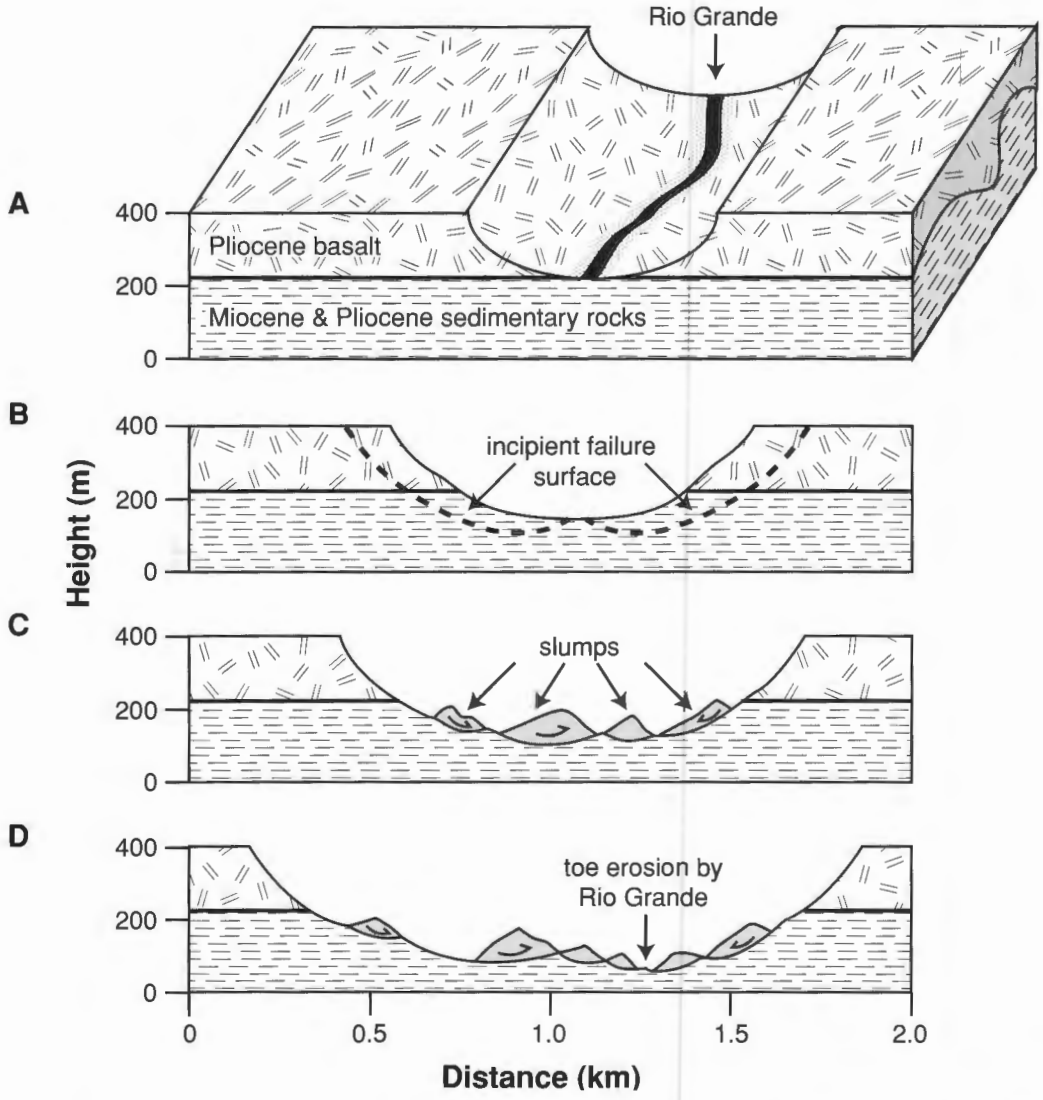

Fig. 26. Schematic long-term evolution of northern White Rock Canyon. (A) Canyon incised entirely into basalt, lacking slump landslides. (B) Continued canyon incision has exposed a section of weaker sediments of sufficient thickness beneath the basalts to allow the initiation of slumps. (C) Rapid retreat of the canyon rims occurs associated with slumping. Erosion of the landslide toes by the Rio Grande generates additional instability, allowing renewed movement of the slumps. The landslides may temporarily dam the Rio Grande. (D) Continued slumping reduces the average canyon wall gradient, reducing the potential for initiation of additional slumps.

has been exposed. Because these assumptions undoubtedly oversimplify actual field conditions, the following approximations should be used cautiously, although they do provide a reasonable framework for considering spatial and temporal variations in landsliding in White Rock Canyon.

The approximate time of initiation of major slump landslides can be estimated for any part of the canyon by using an empirically based threshold for initiation of these landslides as a function of the thickness of exposed sedimentary rocks in combination with the incision history of the Rio Grande. Large areas of slump landslides are not present downriver of Chaquehui Canyon, and we therefore make the initial assumption that the 70 m of sediments exposed beneath basalts at Chaquehui Canyon represents a minimum threshold thickness for initiation of major slumps. Although the detailed post-Bandelier Tuff incision history of White Rock Canyon is not well constrained, approximations can be made based on data collected elsewhere in the region. The best data on incision of the major rivers in northern New Mexico have been obtained further north in the Española basin (Dethier et al., 1988, 1990; Dethier and McCoy, 1993) where about 110 m of incision has occurred along the Rio Chama since eruption of the Lava Creek B tephra 620 ka, for an average long-term incision rate of 0.18 m/ky (meters per thousand years). Possible correlative alluvial surfaces downriver in the Cochiti Dam area are similarly located about 90 to 150 m above the Rio Grande (Dethier et al., 1988), so as a first approximation we estimate that the river has incised 120 ± 30 m in White Rock Canyon since 620 ka at an average long-term rate of 0.19 ± 0.05 m/ky. By using this rate and elevations of the lower basalts along the canyon walls, we can estimate when 70 m of sediments was exposed at different sites. Table 5 presents estimates of the time that slumps may have been initiated in different parts of White Rock Canyon, based on these assumptions.

The assumptions made in Table 5 greatly oversimplify the controls on slope stability in White Rock Canyon and thus only suggest the general time scales that may be involved. In addition to uncertainties involving the incision rate, variations in the strength of the sedimentary rocks will affect the timing of initial failure. For example, the strength of ancestral Rio Grande gravels is probably relatively high and the strength of clay-rich lacustrine sediments relatively low; threshold thicknesses for slump initiation therefore could be significantly lower in the lacustrine sediments, resulting in earlier initiation of slumps. Slope stability is also strongly influenced by pore water pressures, which are related to the location and elevation of groundwater discharge. Thresholds for failure might be lowest in areas of highest groundwater discharge, although discharge variations along White Rock Canyon are not well constrained. Despite these uncertainties concerning thresholds for slumping, the estimates in Table 5 illustrate that slump landslides may have been occurring in White Rock Canyon for hundreds of thousands of years and that this style of failure may have been initiated significantly earlier upcanyon than in the TA-33 area. These time scales are also reasonable in light of the age constraints discussed earlier.

The estimates of the time of landslide initiation, T_0, in Table 5 can be combined with data on the width of the modern canyon, W_m (Fig. 13), and approximations of the canyon width at time of landslide initiation, W_0, to calculate approximate average rates of canyon widening or rates of canyon rim retreat, R:

$$R = (W_m - W_0)/T_0.$$

An estimate of the width of the canyon at the initiation of major slump landslides is provided by the relationship between canyon width and canyon depth shown in Fig. 27, which includes data from both the

TABLE 5
POSSIBLE TIME OF INITIATION OF MAJOR SLUMP LANDSLIDES IN WHITE ROCK CANYON

Site	Elevation of Base of Basalt (ft) *	Rio Grande Elevation (ft)	Thickness of Sedimentary Rocks (ft/m)	Time of Initiation of Major Slumps ** Best Estimate (ka)	Range (ka)
Chaquehui Canyon	5600	5370	230/70	-	-
Ancho Canyon	5710	5380	330/100	160	125-215
Water Canyon	5750	5390	360/110	210	165-285
Mortandad Canyon	5850	5440	410/125	290	230-395
SW of Otowi Bridge	6010	5480	530/160	475	375-645

Notes:
* From Dethier (1995).
** Assumes constant incision rate of 0.19 ± 0.05 m/ky, and initiation of slumps after 70 m of sedimentary rocks have been exposed.

modern canyon in basalt and the early Quaternary canyon. Variations in canyon stratigraphy, the estimated time of landslide initiation, canyon width, and canyon rim retreat rates, based on the above approximations, are shown in Fig. 28. Estimated average rim retreat rates in areas of slumping are generally 1 to 4 m/ky (Fig. 28d). These rates are up to an order of magnitude higher than rates of 0.37 m/ky predicted using the canyon width-to-depth relation in Fig. 27 and an incision rate of 0.19 m/ky; they illustrate the major increase in erosion rates of the canyon rims that would occur once slumps are initiated.

Note that several parts of White Rock Canyon have modern widths similar to what would be expected if the slopes were entirely underlain by basalt, particularly the Overlook and Mortandad Canyon areas and an area southwest of Otowi bridge (Fig. 28c). The canyon width at MDA-D is notably no wider than expected from a site exposing no underlying sediments. These locations could be expected to be the most susceptible to future failure, which is consistent with the interpretation made earlier based solely on average canyon slope gradients (Fig. 14).

The estimated average rim retreat rates shown in Fig. 28d should be considered approximate because of the numerous underlying assumptions. However, several points are worth noting. Significant local variations in estimated average widening rate are shown in Fig. 28d, illustrating the spatial variability in past landsliding along the northwest slopes of White Rock Canyon. In addition, the estimated widening rate generally increases downriver, despite the fact that the mechanically weakest rocks, the Pliocene lacustrine sediments, are only present upriver. This apparent downriver increase in rim retreat rate may reflect a combination of two tendencies. First, the scale of the landsliding, specifically the width of individual slide blocks (measured perpendicular to the canyon rim), may generally increase downriver associated with the increase in thickness of basalt, and thus the accompanying increase in minimum slide depth. Second, the rate of canyon widening at each site may decrease over time, as the initiation of large slumps acts to both decrease the average canyon wall gradient and to buttress the lower slopes, possibly inhibiting new rim failures. Renewed rim failures may require both significant erosion of the landslide toe, such as occurred in the late Pleistocene in the Water Canyon

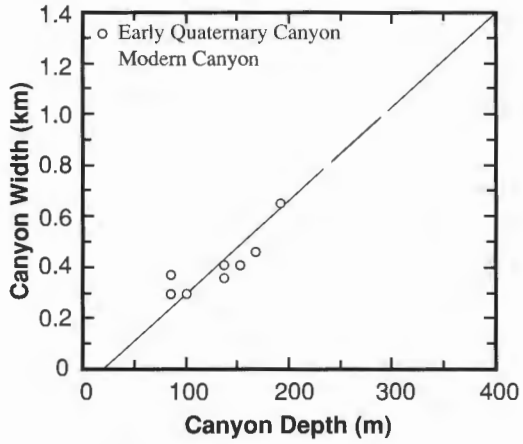

Fig. 27. Plot of canyon width vs. canyon depth for parts of the modern White Rock Canyon incised primarily into basalt and for the early Quaternary Rio Grande canyon. Width (m) = 3.88 * depth (m) - 0.08 (r^2 = 0.89).

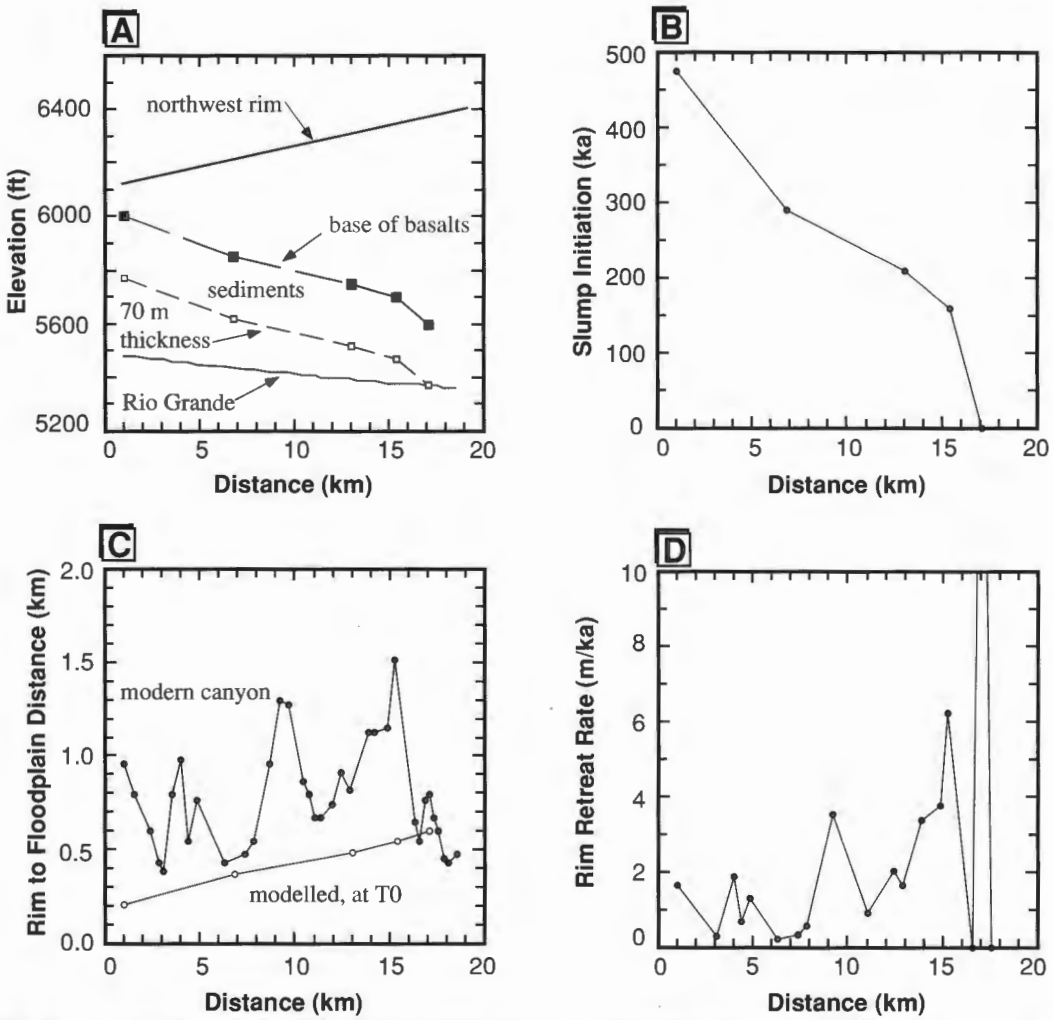

Fig. 28. (A) Approximate variations in stratigraphy along northwest side of White Rock Canyon. Sediments may include Santa Fe Group, Puye Formation, Pliocene alluvium, and Cerros del Rio maar deposits. (B) Time of initiation of major slump landslides using "best estimates" of Table 5. (C) Modern canyon rim-to-floodplain distance and estimated distance at time in (B). (D) Estimated average rim retreat rate since time of initiation of slumps for northwest side of White Rock Canyon. Horizontal axes are distance downstream from Otowi bridge.

West slump complex, and significant canyon incision. For example, using the estimated incision rate of 0.19 ± 0.05 m/ky for the Rio Grande indicates that an average of 40 to 70 ky would be required for 10 m of incision; however, for a slope 260 m high and 1.2 km long, as at the Water Canyon West slump complex, this would increase the average slope gradient by only about 5%, from 0.22 to 0.23. After initiation of major slumping at a site, it is possible that renewed failure of the rim may be inhibited for hundreds of thousands of years, although this inference is necessarily speculative.

IMPLICATIONS FOR POTENTIAL SLOPE INSTABILITY AT MDAS

Landslide characteristics discussed in the preceding sections allow us to infer whether slope failures could be sufficient to expose buried waste at the TA-33 MDAs over time periods of at least 10s to 1000s of years. Spatial relations of landsliding to bedrock variations and data on the timing and frequency of failure are particularly important. These observations indicate that the exposure of buried wastes at MDA-E by mass-wasting over these time periods is improbable. The stability of MDA-D and other contaminated areas at East Site is more problematic because several lines of evidence suggest that the mesa at East Site is potentially susceptible to large-scale slump failures such as those that are present in adjacent areas. Uncertainties exist concerning the triggering mechanisms for such slumps, including the possibility of seismic triggers, but available data suggest that initiation of the largest slumps may require significantly wetter climatic conditions than at present, such as those that characterized the period from about 12 to 20 ka. The probability of similar climatic conditions recurring in the next 100s to 1000s of years is unknown, and thus a more complete evaluation of the potential for failure at MDA-D over these time scales is not possible. These lines of evidence are discussed below.

Influence of Rock Type on Mass-Wasting

The extensive slump complexes exposed along White Rock Canyon from Otowi bridge to the vicinity of TA-33 involve failure of Pliocene basalts overlying weaker Pliocene and Miocene sedimentary rocks. Massive landslides occur only after canyons are incised through basalts, exposing a thick section of the underlying weak rock units. A major change in canyon morphology occurs at TA-33. The canyon is wide upstream, where it averages 1.8 km between canyon rims and is characterized by extensive landslide complexes; downstream the canyon is narrower (averaging <1.0 km), and displays smaller and more restricted landslides. This change in canyon morphology corresponds to a change in rock types. Pliocene alluvial and lacustrine deposits, Santa Fe Group sediments, and altered zones in the Puye Formation fanglomerate, the three units most clearly associated with massive slope failures to the north, become thin or absent south of Chaquehui Canyon. Some phreatomagmatic deposits exposed to the south are sufficiently weak to produce slumping, but the scale of failure is relatively small. At MDA-E, Chaquehui Canyon has not yet cut deeply enough to expose any sedimentary units beneath the basalt (Fig. 5b), and initiation of slumps as seen in White Rock Canyon proper is thus unlikely. However, the MDA-D area appears to be susceptible to slump failures, which is indicated by the occurrence of slumps both upriver and downriver (i.e., Figs. 11 and 12; Plate 1).

We conclude that it is improbable that small-scale rockfalls involving primarily Bandelier Tuff will be sufficient to expose buried wastes at either MDA-E or MDA-D. No evidence of the failure of significant portions of the mesa rim (>5 m into the mesa) was seen. Instead, mass-wasting of the mesa edges seems restricted to relatively small (0-to-4 m wide) rockfalls, as has been

observed in other parts of the Pajarito Plateau. The largest landslides in Bandelier Tuff at TA-33 occur within Chaquehui Canyon immediately downstream of MDA-E where an exceptionally thick section of tuff (>100 m) is exposed within a pre-Bandelier Tuff paleocanyon (Fig. 5b). The occurrence of these large Bandelier Tuff failures in Chaquehui Canyon is consistent with observations made elsewhere on the Pajarito Plateau, such as at Los Alamos and Pajarito Canyons, where partially detached blocks (>15 m into the mesas) occur along canyons exceeding 60 m in depth (Reneau, 1994, 1995). At MDA-E and MDA-D, thinner sections of tuff are present (50 m thick, Fig. 5), and the thickness of the tuff is apparently insufficient to allow large-scale failure. The disposal pits at MDA-E are about 20 m from the mesa edge at their closest point, and a minimum of 4 to 5 individual rockfalls would be required to expose material within these pits.

Local Susceptibility to Mass-Wasting

Within the part of White Rock Canyon characterized by large-scale slump landslides, specifically upriver from Chaquehui Canyon, variations in local topography allow inferences to be made about the relative susceptibility of different parts of the canyon to future slump initiation. Shear stress at the base of a slope increases with increasing slope gradient, and, all other factors being equal, the least stable areas are those with the steepest gradient. Along the northwest side of White Rock Canyon, four areas stand out as having significantly higher average slope gradients: an area about 3 km downriver from Otowi bridge; the MDA-D area; the White Rock Overlook area; and, to a lesser degree, the Water Canyon East slump complex (Fig. 14). No lithologic variations sufficient to imply greater resistance to landsliding were observed at these areas, although the bedrock is generally obscured beneath colluvium and landslide debris. In addition, springs occur in some of these areas, including the Overlook area and the MDA-D area (Purtymun et al., 1980), suggesting that the stability of these areas cannot be argued because of the absence of groundwater discharge. Based on these observations, all four areas could be considered particularly susceptible to future slump initiation.

Timing of Mass-Wasting

The age of landslides and other mass movement deposits provide critical data for evaluating the frequency and triggering mechanisms of failure. The largest mass movement deposits in White Rock Canyon are overlain by the El Cajete pumice, documenting that these failures are older than 58 ka years in age. These old deposits include the narrow slumps below TA-33 between Chaquehui Canyon and Ancho Canyon, the massive rock avalanche deposit north of Ancho Canyon, and the series of massive slump complexes extending from south of Water Canyon to north of White Rock.

Significant landslide activity during the time period after eruption of the El Cajete pumice, >58 ka, has been documented at several locations in White Rock Canyon. The youngest landslides include sites in Mortandad Canyon, that are underlain by Pliocene lacustrine deposits and are in areas of spring discharges. Recent movement at the Mortandad Canyon site was apparent during the spring of 1993, possibly related to the relatively high precipitation that occurred during the winter of 1992-1993. The susceptibility of Santa Fe Group sediments to failure following toe erosion even under modern climatic conditions is indicated by recurring movement of one landslide along State Route 4 immediately east of Otowi bridge where the toe was steepened during highway widening. Similar small-scale movement caused by toe erosion by the Rio Grande has also been seen in White Rock Canyon.

Closer to TA-33, the most recent large landslide failures that have been recognized are in the Water Canyon West slump complex. At this side, the toe of a large pre-El Cajete slump was apparently reactivated several times in the late Pleistocene, damming the Rio Grande and creating lakes. At least four damming events are inferred in the period between about 12 and 18 ka. These ages correspond to the time of the most recent glaciation and to the transition to the succeeding interglacial period, a period significantly wetter than today, and strongly suggest that triggering of the landslides was associated with these different climates. The reactivation of the landslides could have been triggered by several possible mechanisms and was perhaps related to either increased groundwater discharge from the aquifer beneath the Pajarito Plateau or to lateral cutting or incision by the Rio Grande associated with significantly higher flood discharges. Importantly, these ages are older than the last large earthquakes that have been documented on the Pajarito Plateau (Magnitude 6.5 to 7 earthquakes about 4 to 6 ka and 8 to 9 ka; Gardner et al., 1990; Wong et al., 1993), suggesting that seismic shaking in the absence of wet antecedent conditions is inadequate for the triggering of slumping.

The apparent association of movement within the White Rock Canyon slump complexes and the wetter late Pleistocene climate suggests that similar climatic conditions were associated with the older slumping and would be required for the initiation of future large-scale slumps. Significantly, as the largest White Rock Canyon slumps pre-date the >58-ka El Cajete pumice, no evidence has been seen for slump initiation during the wetter period of the latest Pleistocene, including in the four areas inferred to be most susceptible to failure (discussed above). Major landsliding in the latest Pleistocene has instead been recognized only at the toes of slump complexes. These observations imply that wet climatic conditions may be necessary but not sufficient to trigger major landsliding in White Rock Canyon and that new rim failures, including at MDA-D, may similarly not occur during the next wet climatic period.

Summary

Available data on the distribution, ages, and causes of mass-wasting in the vicinity of TA-33 indicate that exposure of buried wastes at MDA-E by mass-wasting over time periods of 10s to 1000s of years is improbable. Rock units underlying MDA-E and exposed in the walls of Chaquehui Canyon, consisting of about 50 m of Bandelier Tuff overlying 50 m of basalt, are much less susceptible to failure than other units exposed in White Rock Canyon. Mass-wasting of the mesa edge adjacent to MDA-E appears restricted to infrequent, small-scale rock falls from the cliffs that would involve blocks less than 5 m in size and exposure of wastes buried 20 m or more from the mesa edge would require a minimum of 4 to 5 individual rockfall events.

MDA-D and adjacent areas at East Site are inferred to have a higher potential for exposure of contaminants by landsliding because of the nearby presence of massive slumps and the relatively steep canyon walls. The most likely trigger for such slumps is inferred to be either a significant increase in groundwater discharge rates or erosion of the toe of the slope by the Rio Grande during periods of higher flood discharges. Both mechanisms probably require significantly wetter climates than those of today, such as the climates that would accompany the next period of major continental glaciation. However, reliable predictions of the timing of new slumps at East Site are not possible, and the observation that these areas were stable through wetter periods in the latest Pleistocene provides evidence that they may also remain stable through future wet periods.

ACKNOWLEDGMENTS

This work was supported by the Environmental Restoration Program of Los Alamos National Laboratory, as part of site characterization activities for Operable Unit 1122 and the Framework Studies program within the Earth Science Technical Team. The authors thank Keith Dowler, Dorothy Hoard, Bill Laughlin, and Roy Michelotti, with OU 1122, and Jamie Gardner, Earth Science Technical Team, for their support; Kirk Anderson and Antonio Garcia for field assistance; Doug Walther and Liz Zeiler for map production; Barry Moore for drafting assistance; and Kirk Anderson, Dave Broxton, and Bill Laughlin for helpful review comments.

REFERENCES CITED

Allen, B.D., 1991, Effect of climatic change on Estancia Valley, New Mexico: Sedimentation and landscape evolution in a closed-drainage basin: in Julian, B., and Zidek, J., Field Guide to Geologic Excursions in New Mexico and Adjacent Areas of Texas and Colorado, *New Mexico Bureau of Mines and Mineral Resources Bulletin* 137, p. 166-171.

Allen, B.D., and Anderson, R.Y., 1993, Evidence from western North America for rapid shifts in climate during the last glacial maximum: *Science*, v. 260, p. 1920-1923.

Aubele, J.C., 1978, Geology of Cerros del Rio volcanic field: in Hawley, J.W., ed., Guidebook to Rio Grande Rift in New Mexico and Colorado, *New Mexico Bureau of Mines and Mineral Resources Circular* 163, p. 198-201.

Bachhuber, F.W., 1989, The occurrence and paleolimnologic significance of cutthroat trout (*Oncorhynchus clarki*) in pluvial lakes of the Estancia basin, central New Mexico: *Geological Society of America Bulletin*, v. 101, p. 1543-1551.

Bailey, R. A., Smith, R. L., and Ross, C. S., 1969, Stratigraphic nomenclature of volcanic rocks in the Jemez Mountains, New Mexico: in Contributions to Stratigraphy, *U.S. Geological Survey Bulletin* 1274-P, p. 1-18.

Baltz, E. H., Abrahams, J. H., and Purtymun, W. D., 1963, Preliminary report on the geology and hydrology of Mortandad Canyon near Los Alamos, New Mexico, with reference to disposal of liquid low-level radioactive waste: U.S. Geological Survey Open File Report, Albuquerque, New Mexico.

Bierman, P.R., and Gillespie, A.R., 1994, Evidence suggesting that methods of rock-varnish cation-ratio dating are neither comparable nor consistently reliable: *Quaternary Research*, v. 41, p. 82-90.

Birkeland, P. W., 1984, Soils and Geomorphology: Oxford, New York, 372 p.

Bowen, B. M., 1990, Los Alamos Climatology: Los Alamos National Laboratory Report LA-11735-MS, Los Alamos, New Mexico, 254 p.

Campbell, C.S., 1989, Self-lubrication for long runout landslides: *Journal of Geology*, v. 97, p. 653-665.

Dethier, D.P., 1993a, Geology of Northern White Rock Canyon, New Mexico: unpublished report for Los Alamos National Laboratory under subcontract 9-LC3-6519F-1, 26 p.

Dethier, D.P., 1993b, Landslides and Other Mass Movements Near TA-33, Northern White Rock Canyon, New Mexico: Final Report for Los Alamos National Laboratory under subcontract 9-LC3-6519F-1, 34 p.

Dethier, D.P., 1995, Geologic map of the White Rock quadrangle: New Mexico Bureau of Mines and Mineral Resources, in press.

Dethier, D. P., and McCoy, W. D., 1993, Aminostratigraphic relations and age of Quaternary deposits, northern Española basin, New Mexico: *Quaternary Research*, v. 39, p. 222-230.

Dethier, D.P., Harrington, C.D., and Aldrich, M.J., 1988, Late Cenozoic rates of erosion in the western Española basin, New Mexico: Evidence from geologic dating of erosion surfaces: *Geological Society of America Bulletin*, v. 100, p. 928-937.

Dethier, D.P., Halverson, N., Marrack, L., Meagher, M., Oelkers, E., Harrington, C.D., Sarna-Wojcicki, A., and Meyer, C.E., 1990, Occurrence of the Lava Creek B tephra layer in the northwestern Española Basin, New Mexico: *New Mexico Geology*, v. 12, p. 77-82.

Dransfield, B.J., and Gardner, J.N., 1985, Subsurface geology of the Pajarito Plateau, Española Basin, New Mexico: Los Alamos National Laboratory Report LA-10455-MS, 15 p.

Elias, S.A., Carrara, P.E., Toolin, L.J., and Jull, A.J.T., 1991, Revised age of deglaciation of Lake Emma based on new radiocarbon and macrofossil analyses: *Quaternary Research*, v. 36, p. 307-321.

Galusha, T., and Blick, J.C., 1971, Stratigraphy of the Santa Fe Group, New Mexico: *American Museum Natural History Bulletin 144*, 127 p.

Gardner, J.N., and House, L., 1987, Seismic hazard investigations at Los Alamos National Laboratory, 1984-1985: Los Alamos National Laboratory Report LA-11072-MS, 76 p.

Gardner, J. N., Baldridge, W. S., Gribble, R., Manley, K., Tanaka, K., Geissman, J. W., Gonzalez, M., and Baron, G., 1990, Results from Seismic Hazards Trench #1 (SHT-1), Los Alamos Seismic Hazards Investigations: Los Alamos National Laboratory Memorandum EES1-SH90-19, Los Alamos, New Mexico.

Graf, W.L., 1994, Plutonium in the Rio Grande: New York, Oxford University Press, 329p.

Griggs, R.L., 1964, Geology and groundwater resources of the Los Alamos area, New Mexico: U.S. Geological Survey Water-Supply Paper 1735, 107 p.

Heiken, G., Goff, F., Stix, J., Tamanyu, S., Shafiqullah, M., Garcia, S., and Hagan, R. C., 1986, Intracaldera volcanic activity, Toledo caldera and embayment, Jemez Mountains, New Mexico: *Journal of Geophysical Research,* v. 91, p. 1799-1815.

Heiken, G., Wohletz, K., Fisher, R.V., and Dethier, D.P., 1995, Maar volcanoes of White Rock Canyon—Interaction of ground and surface water with basaltic volcanoes of the Rio Grande rift, New Mexico: Field Trip 21 I of the 1989 IAVCEI General Assembly, June 25-July 1, 1989, Santa Fe: New Mexico Geological Society Field Trip Guidebook (in press)

Hsu, K.J., 1975, Catastrophic debris streams (Sturzstroms) generated by rockfalls: *Geological Society of America Bulletin*, v. 86, p. 129-140.

Izett, G.A., and Obradovich, J.D., 1994, $^{40}Ar/^{39}Ar$ age constraints for the Jaramillo Normal Subchron and the Matuyama-Brunhes geomagnetic boundary: *Journal of Geophysical Research*, v. 99 (B2), p. 2925-2934.

Jibson, R.W., and Keefer, D.K., 1993, Analysis of the seismic origin of landslides: Examples from the New Madrid seismic zone: *Geological Society of America Bulletin*, v. 105, p. 521-536.

Keefer, D. K., 1984, Landslides caused by earthquakes: *Geological Society of America Bulletin*, v. 95, p. 406-421.

Keefer, D. K., and Wilson, R. C., 1989, Predicting earthquake-induced landslides, with emphasis on arid and semi-arid environments, *in* Landslides in a Semi-Arid

Environment, With Emphasis on the Inland Valleys of Southern California, edited by P. M. Sadler and D. M. Morton. *Publications of the Inland Geological Society,* v. 2, p. 118-149.

LANL, 1992, RFI Work Plan for Operable Unit 1122, Environmental Restoration Program: Los Alamos National Laboratory report LA-UR-92-925.

Laughlin, A.W., Woldegabriel, G., and Dethier, D., 1993, Preliminary Report, FY93, Volcanic Stratigraphy of the Pajarito Plateau: unpublished report for Los Alamos National Laboratory, Los Alamos, New Mexico.

Luedke, R.G., and Smith, R.L., 1978, Map showing distribution, composition and age of late Cenozoic volcanic centers in Arizona and New Mexico: U.S. Geological Survey Miscellaneous Investigations Map I-1091A.

Machette, M.N., 1985, Calcic soils of the southwestern United States, in Weide, D.L., ed., Soils and Quaternary Geology of the Southwestern United States: Geological Society of America Special Paper 203, p. 1-21.

Nicoletti, P.G., and Sorriso-Valvo, M., 1991, Geomorphic controls of the shape and mobility of rock avalanches: *Geological Society of America Bulletin*, v. 103, p. 1365-1373.

Nordin, C. F., Jr., and Beverage, J. P., 1965, Sediment transport in the Rio Grande, New Mexico: U.S. Geological Survey Professional Paper 462-F, 35 p.

Phillips, F.M., Peeters, L.A., Tansey, M.K., and Davis, S.N., 1986, Paleoclimatic inferences from an isotopic investigation of groundwater in the central San Juan Basin, New Mexico: *Quaternary Research*, v. 26, p. 179-193.

Phillips, F.M., Campbell, A.R., Kruger, C., Johnson, P., Roberts, R., and Keyes, E., 1992, A reconstruction of the response of the water balance in western United States lake basins to climatic change: New Mexico Water Resources Research Institute Report No. 269, Las Cruces, New Mexico, v. 1, 167 p.

Porter, S.C., Pierce, K.L., and Hamilton, T.D., 1983, Late Wisconsin mountain glaciation in the western United States: in Porter, S.C., ed., Late-Quaternary Environments of the United States, Vol. I, The Late Pleistocene, p. 71-111.

Purtymun, W. D., Peters, R. J., and Owens, J. W., 1980, Geohydrology of White Rock Canyon of the Rio Grande from Otowi to Frijoles Canyon: Los Alamos Scientific Laboratory Report LA-8635-MS, 15 p.

Reneau, S.L., 1995, Geomorphic characterization of Technical Area 21, Los Alamos National Laboratory, New Mexico: *in* Earth Science Investigations to Support Environmental Restoration at Los Alamos National Laboratory Technical Area 21, Los Alamos National Laboratory Report LAUR LA-12934-MS, p. D1-D29.

Reneau, S.L., 1994, Potential Mesa-Edge Instability at Pajarito Mesa, Los Alamos National Laboratory, New Mexico: unpublished report, Los Alamos National Laboratory, Los Alamos, New Mexico.

Reneau, S.L., and Raymond, R., Jr., 1991, Cation-ratio dating of rock varnish: Why does it work?: *Geology*, v. 16, p. 937-940.

Richmond, G.M., 1986, Stratigraphy and correlation of glacial deposits of the Rocky Mountains, the Colorado Plateau and the ranges of the Great Basin: in Sibrava, V., Bowen, D.Q., and Richmond, G. M., eds., Quaternary Glaciations in the Northern Hemisphere, Report of the International Geological Correlation Programme Project 24, Pergamon Press, Oxford, p. 99-127.

Selby, M.J., 1982, Hillslope Materials and Processes: Oxford University Press, Oxford, 264 p.

Self, S., Kircher, D.E., and Wolff, J.A., 1988, The El Cajete Series, Valles Caldera, New Mexico: *Journal of Geophysical Research*, v. 93 (B6), p. 6113-6127.

Self, S., Wolff, J.A., Spell, T.L., Skuba, C.E., and Morrissey, M.M., 1991, Revisions to the stratigraphy and volcanology of the post-0.5 Ma units and the volcanic section of VC-1 core hole, Valles caldera, New Mexico: *Journal of Geophysical Research*, v. 96 (B3), p. 4107-4116.

Spaulding, W. G., 1992, Late Quaternary paleoclimates and sources of paleoenvironmental data in the vicinity of Los Alamos National Laboratory—Final Report: unpublished report for Los Alamos National Laboratory by Dames and Moore, Las Vegas, Nevada, 32 p.

Spaulding, W. G., Leopold, E.B., and Van Devender, T.R., 1983, Late Wisconsin paleoecology of the American Southwest: in Porter, S.C., ed., Late-Quaternary Environments of the United States, Vol. I, The Late Pleistocene, p. 259-293.

Spiegel, Z., and Baldwin, B., 1963, Geology and water resources of the Santa Fe area, New Mexico: U.S. Geological Survey Water-Supply Paper 1525, 258 p.

Stuiver, M., and Reimer, P. J., 1993, Extended ^{14}C data base and revised CALIB 3.0 ^{14}C age calibration: *Radiocarbon*, v. 35, p. 215-230.

Toyoda, S., Goff, F., Ikeda, S., and Ikeya, M., 1995, ESR dating of quartz phenocrysts in the El Cajete and Battleship Rock Members of Valles Rhyolite, Valles Caldera, New Mexico: *Journal of Volcanology and Geothermal Research* (in press).

Van Devender, T.R., Thompson, R.S., and Betancourt, J.L., 1987, Vegetation history of the deserts of southwestern North America; The nature and timing of the Late Wisconsin-Holocene transition, in Ruddiman, W.F., and Wright, H.E., Jr., eds., North America and adjacent oceans during the last deglaciation: Boulder, Colorado, Geological Society of America, The Geology of North America, v. K-3, p. 323-352.

Vaniman, D., and Wohletz, K., 1990, Results of geological mapping/fracture studies: TA-55 area: Los Alamos National Laboratory Memorandum EES1-SH90-17, Los Alamos, New Mexico, 23 p.

Varnes, D.J., 1978, Slope movement types and processes: in Schuster, R.L., and Krizek, R.J., eds., Landslides, Analysis and Control: Transportation Research Board Special Report 176, p. 12-33.

Waresback, D. B. and Turbeville, B.N., 1990, Evolution of a Plio-Pleistocene volcanogenic alluvial fan: The Puye Formation, Jemez Mountains, New Mexico: *Geological Society of America Bulletin*, v. 102, p. 298-314.

Watchman, A., 1992, Doubtful dates for Karolta engravings: *Australian Aboriginal Studies* 1992, no. 1, p. 51-55.

Watchman, A., 1994, Investigating the cation-ratio calibration curve: Evidence from South Australia: *Rock Art Research* (in press).

Wong, I., Hemphill-Haley, M., Kolbe, T., Green, R., Bott, J., Kanakari, H., Kelson, K., Haraden, C., Gardner, J., House, L., Reneau, S., Keller, D., Silva, W., and Stark, C., 1993, Deterministic and probabilistic seismic hazard evaluation of the Los Alamos National Laboratory: Proceedings of Fourth DOE Natural Phenomena Hazards Mitigation Conference, Atlanta, GA, DOE Report CONF-9310102, v. 1, p. 258-267.

This report has been reproduced directly from the
best available copy.

It is available to DOE and DOE contractors from the
Office of Scientific and Technical Information,
P.O. Box 62,
Oak Ridge, TN 37831.
Prices are available from
(615) 576-8401.

It is available to the public from the
National Technical Information Service,
US Department of Commerce,
5285 Port Royal Rd.
Springfield, VA 22161.

Geology of OU 1122

LEGEND

- Boundary, LANL
- Boundary, OU
- Contours, 10 Foot
- Contours, 100 Foot
- Geologic Contact
- Geologic Contact, Approximate
- Material Disposal Area
- Roads, Dirt
- Roads, Paved
- Road/Trail

- f artificial fill
- Qa3 Alluvial deposits (Holocene and Pleistocene)
- Qa2 Alluvial and lacustrine deposits (late Pleistocene)
- Qf3 Alluvial fan deposit (Holocene and late Pleistocene)
- Qf2 Alluvial fan deposit (late Pleistocene)
- Qf1 Alluvial fan deposit (middle Pleistocene)
- Qt Talus deposit (Holocene and late Pleistocene)
- Qc Colluvial deposits (middle Pleistocene to Holocene)
- Qls Landslide deposit (Pleistocene)
- Qlsa Alluvial and colluvial deposits on landslides (Pleistocene)
- Qec El Cajete pumice (late Pleistocene)
- Qbt-3 Bandelier Tuff, Tshirege member, Unit 3 (early Pleistocene)
- Qbt-2 Bandelier Tuff, Tshirege member, Unit 2 (early Pleistocene)
- Qbt-1 Bandelier Tuff, Tshirege member, Unit 1 (early Pleistocene)
- Qbt Bandelier Tuff, Tshirege member, undivided (early Pleistocene)
- Qao Early Pleistocene alluvium
- Qbo Bandelier Tuff, Otowi member (early Pleistocene)
- Tpf Puye Formation, fanglomerate facies (Pliocene)
- Tpt Puye Formation, ancestral Rio Grande facies (Pliocene)
- Tcc Cinder cone deposit (Pliocene)
- Tcm Phreatomagmatic deposit (Pliocene)
- Tcb3 Tholeiitic basalt flows (late Pliocene)
- Tcba Basaltic andesite and related flows (Pliocene)
- Tcbm Basalt flows and interlayered phreatomagmatic deposits (Pliocene)
- Tcb2 Basalt flows (Pliocene)
- Tcb1 Basaltic flows (Pliocene)
- Tcbu Basalt flows, undivided (Pliocene)
- Tsfu Santa Fe Group, undivided (middle Miocene to early(?) Pliocene)
- Gully
- Rockfall
- Sample location
- Fault, bar and ball on downthrown side
- Scarp of partially detached landslide block
- Strike and dip
- Pressure ridge on rock avalanche

4720

Plate 1 of "Landslides and Other Mass Movements Near Technical Area 33, Los Alamos National Laboratory". Los Alamos National Laboratory Report LA-12955-MS.

Modified from Dethier (in press), "Geologic Map of White Rock Quadrangle".

Mapping by D. P. Dethier (1985-86, 1993) and S. L. Reneau (1993-94)

N

State Plane Coordinate System, New Mexico Central Zone. 1983 North American Datum

Contour Interval = 10 feet

Feet per inch on map = 500

SCALE 1:6000

0 152 304 456 608

METERS

0 500 1000 1500 2000

FEET

NOTICE: The information on this map is provisional. Feature locations are dependent on scale and projection and their accuracy and completeness are not guaranteed. Los Alamos National Laboratory boundary is based on legal descriptions established in 1995. Other boundary, structure and utility data are from Los Alamos National Laboratory Engineering Division and Los Alamos County Utility and Engineering Departments. Contour data are from Los Alamos National Laboratory Environmental Restoration Project aerial survey, September, 1991.

University of California

Los Alamos National Laboratory

Earth and Environmental Sciences Division

FIMAD Facility for Information Management, Analysis and Display
FIMAD is the electronic data repository for the Environmental Restoration Project at Los Alamos National Laboratory.

Produced by: Doug Walther

Date: April 29, 1995 FIMAD Plot ID: G103376

LOCATION OF OU 1122

1744100

1741100

1738100

1735100

1732100

1635500

1638500

1641500

1644500

1647500

1650500

1653500

FIMAD 29 Apr 95